



Supplementary Information for

Dental data challenge the ubiquitous presence of *Homo* in the Cradle of Humankind

Clément Zanolli^{a,*}, Thomas W. Davies^{b,c}, Renaud Joannes-Boyau^{d,e}, Amélie Beaudet^{f,g,h}, Laurent Bruxelles^{g,i,j}, Frikkie de Beer^{k,l}, Jakobus Hoffman^k, Jean-Jacques Hublin^b, Kudakwashe Jakata^m, Lazarus Kgasi^{e,n}, Ottmar Kullmer^{o,p}, Roberto Macchiarelli^{q,r}, Lei Pan^{s,t,1}, Friedemann Schrenk^{o,p}, Frédéric Santos^a, Dominic Stratford^q, Mirriam Tawaneⁿ, Francis Thackeray^m, Song Xing^{s,t}, Bernhard Zipfel^m, Matthew M. Skinner^{b,c,u},

^aUniv. Bordeaux, CNRS, MCC, PACEA, UMR 5199, 33600 Pessac, France

^bDepartment of Human Evolution, Max Planck Institute for Evolutionary Anthropology, Deutscher Platz 6, 04103 Leipzig, Germany

^cSchool of Anthropology and Conservation, University of Kent, Canterbury CT2 7NZ, UK

^dGeoarchaeology and Archaeometry Research Group (GARG), Southern Cross GeoScience, Southern Cross University, Military Rd, Lismore, 2480, NSW, Australia

^ePalaeo-Research Institute, University of Johannesburg, Gauteng Province, South Africa

^fDepartment of Archaeology, University of Cambridge, Cambridge, United Kingdom

^gSchool of Geography, Archaeology and Environmental Studies, University of the Witwatersrand, Johannesburg, South Africa

^hInstitut Català de Paleontologia Miquel Crusafont, Universitat Autònoma de Barcelona, Barcelona, Spain

ⁱUMR 5608 CNRS, TRACES, Maison de la Recherche, Université Toulouse Jean Jaurès, 5 allées Antonio Matchado, 31058 Toulouse Cedex 9, France

^jINRAP, French Institute for Preventive Archaeological Researches, 561 rue Etienne Lenoir, km delta, 30900, Nîmes, France

^kSouth African Nuclear Energy Corporation SOC Ltd. (Necsa), Pelindaba, South Africa

^lDepartment of Anthropology & Development Studies, University of Johannesburg, Johannesburg, South Africa

^mEvolutionary Studies Institute, University of the Witwatersrand, 1 Jan Smuts Avenue, Braamfontein, Johannesburg 2000, South Africa

ⁿDitsong National Museum of Natural History, Pretoria, South Africa

^oDepartment of Paleoanthropology, Senckenberg Research Institute and Natural History Museum Frankfurt, 60325 Frankfurt, Germany

^pDepartment of Paleobiology and Environment, Institute of Ecology, Evolution, and Diversity, Goethe University Frankfurt, Frankfurt, Germany

^qUMR 7194 CNRS, Muséum National d'Histoire Naturelle, Paris, France

^rDépartement Géosciences, Université de Poitiers, France

^sKey Laboratory of Vertebrate Evolution and Human Origins, Institute of Vertebrate Paleontology and Paleoanthropology, Chinese Academy of Sciences, Beijing, China

^tCAS Center for Excellence in Life and Paleoenvironment, Beijing, China

^uCentre for the Exploration of the Deep Human Journey, University of the Witwatersrand, 1 Jan Smuts Avenue, Braamfontein, Johannesburg 2000, South Africa

¹ Deceased May 2020.

*To whom correspondence may be addressed: Clément Zanolli

Email: clement.zanolli@gmail.com

This PDF file includes:

Supplementary Note 1
Supplementary Note 2
Supplementary Material and Methods
Figures S1 to S13
Tables S1 to S8
SI References

Supplementary Note 1

Context of discovery of the early Homo specimens

The mandible SK 15, which was found in Member 2 of Swartkrans and is the holotype of *Telanthropus capensis* (1), was later assigned to *H. erectus/ergaster* (2). The isolated premolar SK 18a, also from Member 2, was suggested to belong to SK 15 (3), even though the poor preservation of the premolar alveolae in the latter specimen prevents any confirmation. A few other specimens from Swartkrans Member 2 were attributed to *Homo*, including the permanent lower first molar crowns SKX 257 and SKX 258, antimeres of the same individual, and the permanent upper first molar SKX 268 associated with the deciduous upper second molar SKX 267 and fragmentary crown of the permanent upper canine SKX 269 (4). The crushed juvenile cranium SK 27 (5) and the partial cranium SK 847 (6) recovered in the Hanging Remnant of Member 1, as well as the partial juvenile mandible SKX 21204 from Lower Bank of Member 1 are generally considered to represent *H. erectus/ergaster* or *H. habilis* (5–8). The isolated lower third premolar SK 96 also comes from the same Member and was recently suggested to show a morphology resembling that of the Middle Pleistocene taxon *H. naledi* (9). The eleven deciduous and permanent teeth of KB 5223 from the Member 2 or 3 of Kromdraai represent a young individual that was attributed to either *Paranthropus* (7) or *Homo* (10). The site of Drimolen yielded a large assemblage of hominin remains, most of them being attributed to *P. robustus*, while a few specimens, including the four molars DNH 39, DNH 62, DNH 67 and DNH 70, were assigned to *Homo* (11, 12). For Sterkfontein, the specimen StW 151 comes from Member 4 (13). StW 19b and StW 87 are either from Member 4 or 5 (7). The stratigraphic relationship with Members 4 and 5 of the StW 53 infill, in which the eponym specimen was found, is unclear (7, 8, 13). A recent work by Couzens based on spatial modeling of stone artefacts suggests that StW 53 is best related to Member 4 (some breccia from this Member is still present in the southern part of the Type Site where StW 53 was found) (14). Many of the Sterkfontein specimens generally regarded as *Homo* and investigated here come from Member 5 (SE 255, SE 1508, StW 80-81) (2, 15–17). The recently found isolated molar StW 669 comes from an underground chamber (Milner Hall) in Sterkfontein Cave, in deposits that are correlated to Member 5 (18). It has been attributed to *Homo* based on size and external morphology (19). In this study, we also identified the molar Sts 9 coming from either Member 4 or 5 in the eastern area of the Type Site as likely belonging to early *Homo*.

Supplementary Note 2

Analysis of non-metric features of the enamel-dentine junction

Studies based on scoring of dental traits have shown substantial variation for the presence/absence and degree of development of a number of features in post-canine teeth, notably between Pleistocene *Homo* groups and recent modern humans (20, 21). For example in Holocene humans, three-cusped M²s (i.e., lacking the hypocone) are not recorded in Sub-Saharan African populations whereas it occurs more

frequently in western Eurasians (up to 34%) (21). Four-cusped M₂s (i.e., lacking the hypoconulid) are relatively frequent, between 17% and 75% in sub-Saharan groups, and up to 95% in western Eurasian groups (21). In comparison, three-cusped M²s are not recorded in Pleistocene groups so far and four-cusped M₂s are only rarely found in fossil hominins (21).

In the southern African sample investigated here, all the upper molars have the four main dentine horns corresponding to the paracone, protocone, metacone and hypocone. DNH 62 and the upper molars of StW 151 show a lingual cingulum that is only recorded in one *Homo* specimen of our comparative sample (NG0802.1) (22), but is more common in *Australopithecus* (e.g., MLD 44, Sts 21, Sts 52) and *Paranthropus* (e.g., SK 105, SK 831a, SK 832) (Figs. S1-S3). Most of the upper molars show a well-developed hypoparacrista enclosing a small mesial fovea (only DNH 39, DNH 62 and StW 669 do not show any delimitation of a mesial fovea). This feature is recorded on the EDJ of most of the non-*Homo* comparative specimens. The M³s of StW 53 shows a small accessory fovea enclosed by a marked crest at the mesiobuccal corner of the crown, a singular feature that is not found in any other specimen studied here.

All P₃s have a continuous transverse crest at the EDJ level while among the P₄s, only SK 18a (if it is a P₄) and SKX 21204 have one (Figs. S4-S5). The P₃s tend to show a buccolingually narrower occlusal basin than the P₄s, but SK 18a has an intermediate morphology between the P₃ and P₄ shapes, making its metameric assessment challenging. Among the P₃s, StW 80 shows unique morphology, with a high protoconid but minute metaconid dentine horn, and a buccolingually expanded distal fovea (with a marked postprotocristid) compared with the mesial fovea. A hypoconid dentine horn is barely discernible in SK 18a, SKX 21204 and StW 80, while it is slightly more developed in SK 96. The P₄ specimens exhibit a similar overall pattern, but differ in mesiodistal/buccolingual proportions. A small hypoconid dentine horn is detectable in the P₄ of SKX 21204 and a buccal shelf is also visible (Fig. 1). Besides StW 80, the features found in SK 18a, SK 96, StW 87, StW 151 and SKX 21204 are commonly found in each of the three hominin genera of the comparative sample (Figs. S4-S5) and are thus of little taxonomic value.

The EDJ of the lower molars display variable occlusal outlines and central basin shapes (Fig. S6). All the purported *Homo* specimens share with *Australopithecus* and *Paranthropus* the presence of the five main dentine horns corresponding to the protoconid, metaconid, hypoconid, entoconid and hypoconulid. Four teeth show a complete but low mid-trigonid crest (DNH 67, KB 5223, Sts 9 and the left M₃ of SK 15). Three M₁s (KB 5223, SKX 257 and StW 151) show a buccal cingulum-like feature with deep fossae between the protoconid and hypoconid, and between the hypoconid and hypoconulid (Fig. S6).

We analyzed the frequency and development of eight non-metric dental features of the molar EDJ in the comparative sample (Table S6). Compared with *Australopithecus* and *Paranthropus*, Early to Middle Pleistocene *Homo* shows the absence or a low degree of expression of cusp 5 in the M³s, of the Carabelli trait in the M²s, of the distal accessory cusp in the M₃s, and of the protostyloid for all lower molar positions, as well as higher frequency of the lingual accessory cusp (tuberculum intermedium) in the M₁s (Figs. S1-S8; Table S2). In this respect, the M³s of SK 847, StW 19b and both antimeres of StW 53 show a cusp 5, the M²s of StW 669 and SE 1508 do not exhibit a Carabelli trait, only the M₃ of StW 53 does not have a distal accessory cusp, most M₂s and M₃s display no lingual accessory cusp (except DNH 67, SKX 257 and

StW 80), and eight of the twelve lower molars do not express a protostylid at the EDJ. The developed, shelf-like protostylid of the Ms KB 5223 and SKX 257 resembles the morphology seen in australopiths, while such expression is not recorded in any Early to Middle Pleistocene *Homo* specimen (Fig. S6).

Supplementary Material and Methods

Materials

We investigated the EDJ of 37 southern African post-canine teeth that were previously attributed to early *Homo*, as well as of one isolated lower molar, Sts 9, generally attributed to *Australopithecus* but recognized here as *Homo* (SI Appendix, Supplementary Note 1 and Table S1). We compared this assemblage with Late Pliocene to Early Pleistocene southern African australopiths, including the holotypes of *Australopithecus* (Taung 1, representing *A. africanus*) (23) and *Paranthropus* (TM 1517 representing *P. robustus*) (24). The *Australopithecus* specimens included in this study also sample specimens from Makapansgat that were attributed to *A. prometheus*, such as MLD 2 (25). We also used African and Asian Early to Middle Pleistocene *Homo* specimens as reference for the taxon. There are a number of eastern African specimens that could be relevant to compare with purported early *Homo* specimens from South Africa, however, many are unavailable for study, their taxonomic attribution to *Homo* is similarly debated, and/or there is a lack of tissue contrast in tomographic scans between enamel and dentine tissue that prevents imaging of the EDJ. Therefore, a large part of the comparative *Homo* sample also includes late Early Pleistocene to mid-Middle Pleistocene African and Asian specimens (see SI Appendix Table S2).

Methods

All the southern African specimens were scanned using X-ray microtomography with the X-Tek (Metris) XT H225L industrial microCT system at the South African Nuclear Energy Corporation (Necsa; 26), the Nikon Metrology XTH 225/320 LC dual source microCT system at the Evolutionary Studies Institute, or the BIR Actis 300/225 FP or SkyScan 1172 microtomographic scanners of the Max Planck Institute according to the following parameters: 70–135 kV voltage; 60–420 mA current; a 0.5–1.2 mm Cu filter or 0.1–3.6 mm Al filter. The final volumes were reconstructed with an isotropic voxel size of 10–30 µm for isolated teeth and 40–60 µm for jaw fragments. Most of the comparative sample was scanned by X-ray microtomography with similar parameters, except for 11 *H. erectus* teeth (Sangiran 7-3b, 7-3c, 7-3d, 7-13, 7-17, 7-20, 7-26, 7-53, 7-64, 7-65, 7-89) from Sangiran, Indonesia, that were imaged by neutron microtomography at the ANTARES imaging facility located at the FRM II reactor of the Technical University of Munich, Germany (for technical details see ref. 27). The final virtual volumes of these specimens were reconstructed with an isotropic voxel size of ~21 µm. For all specimens, image stacks were imported into Avizo v.8.0 (FEI Visualization Sciences Group), and the images were segmented using semiautomatic procedures and an adaptation of the half-maximum height method (28–30). All the EDJ surfaces were generated using the ‘constrained smoothing’ option.

Non-metric traits at the EDJ were assessed using scoring systems developed in the frame of previous studies to investigate the frequency of the Carabelli’s feature, the upper and lower molar accessory cusps (C5, C6 and C7, protoconule), the mid-trigonid crest and the protostyloid (Table S6). The protoconule, fifth

and sixth cusp dentine horns (UM C5 and UM C6), and Carabelli trait presence/absence and expression in the upper molars were assessed following Ortiz et al. (31):

- Protoconule and UM C5

0 = dentine horn is absent

0.5 = indecisive category

1 = dentine horn is present and very small

2 = dentine horn is small

3 = dentine horn is medium-sized

4 = dentine horn is large

5 = dentine horn is very large

- UM C6

0 = absent

1 = a dentine horn is present

- Carabelli trait

0 = the mesiolingual aspect of cusp 1 is smooth

1 = a groove is present or the lingual cingulum is reduced to one or two short furrows or a single pit which may be fairly deep.

2 = a pit is present or the lingual cingulum decreases further in length and prominence. There are usually between 3-7 vertical furrows on the protocone which sometimes branch at the occlusal end

3 = a small [or medium-sized] Y-shaped depression is present or the cingulum decreases further in length and prominence but the cuspules are larger

4 = a large Y-shaped depression is present or the cingulum is usually shorter in length but carries one or more cuspules which may break the continuity of the furrow

5 = a small dentine horn without a free apex occurs (the distal border of the cusp does not contact the lingual groove separating cusps 1 and 4) or a complete lingual cingulum is present extending from the mesio-buccal corner of the crown traversing the lingual surface of the protocone in an oblique cervical direction and terminating in the occluso-lingual groove.

6: a medium-sized cusp with an attached apex making contact with the medial lingual groove is present

7: a large cusp is present

The lower molar mid-trigonid crest was scored following Bailey et al. (32):

- 0 = absent or weakly expressed ridges on either or both of the mesial cusps.
- 1 = moderately expressed ridges on both protoconid and metaconid dentine horns that do not join at the sagittal sulcus and are widely spaced.
- 2 = presence of a crest whose height dips and/or is much reduced at the sagittal sulcus but remains continuous.
- 3 = presence of a crest that remains high from dentine horn tip to dentine horn tip. There may be only a slight dip at the sagittal sulcus.

The presence/absence and expression of the distal accessory dentine horn (DAC, often referred to as cusp 6 or tuberculum sextum) and of the lingual accessory dentine horn (LAC, generally named cusp 7 or tuberculum intermedium) were scored following Davies et al. (33):

- DAC

absent

interconulid type = can be single, double or triple

hypoconulid type = can be single or double

entoconid type = single

- LAC

absent

interconulid type = single

metaconid type = can be single or double

entoconid type = single

Because of the vast degree of variation of the protostyliid at the EDJ level (34), we simply scored it as follows:

- 0 = absent or very subtle reliefs, sometimes with a groove between the protoconid and hypoconid (no fovea, shelf and/or crest on the buccal aspect of the trigonid)
- 1 = weak expression (whether it is represented by a fovea, shelf and/or crest on the buccal aspect of the trigonid)

2 = marked expression (whether it is represented by a fovea, shelf and/or crest on the buccal aspect of the trigonid).

We used a diffeomorphic surface matching (DSM) approach to analyze the EDJ conformation. This landmark-free, mesh-based approach relies on the construction of average surface models, and the difference between surfaces is interpreted as the amount of deformation needed to align them by using diffeomorphic shape matching (35, 36). The metric of currents used in DSM analyses takes all data points into account and does not assume a point-to-point correspondence between samples which allows direct comparison of surfaces that have different number of sample points (37). Moreover, this metric takes into account the local orientation of a surface (i.e., the normals) to strengthen the measure of shape dissimilarities (this metric does not only measure how distant two surfaces are, but also how their respective local orientations differ) (37). The deformations between surfaces are mathematically modeled as smooth and invertible functions (i.e., diffeomorphisms). From a set of surfaces, an atlas of surfaces is created. The method estimates an average object configuration or mean shape from a collection of object sets (here the EDJ surfaces) and computes the deformations from the mean shape to each specimen. In addition, a set of initial control points located near its most variable parts, and a set of momenta parameterizing the deformations of the mean shape to each individual are estimated (37–42). When comparing a group of closely related taxa (as it is the case here), it is assumed that the inaccuracy (noise) introduced by comparing whole surfaces is small compared to the information that can be extracted (signal). Compared with landmarks, correspondence between surfaces is not strictly homologous. The assumption about signal to noise ratio has been evaluated in previous studies, showing that DSM can distinguish the EDJ of various hominin groups, even better than with landmark-based analyses, suggesting that DSM can offer reliable accuracy and precision, of a similar order than landmark-based analyses (39, 41). For each dental position, the EDJ surfaces decimated to 50000 polygons were manually oriented, then superimposed using the rigid and uniform scale option (corresponding to a shape alignment, removing size) of the ‘Align Surfaces’ module in Avizo v.8.0 (Visualization Sciences Group Inc.). This was done by minimizing the root mean square distance between the points of each specimen to corresponding points on the reference surface using an iterative closest point algorithm. We used the Deformetrica v. 4.3 software (<https://www.deformetrica.org>) (36, 37) to generate a global mean shape (GMS) with a set of diffeomorphisms relating the GMS to each individual and the output (control points and deformation momenta) used to perform the statistical analyses to explore the EDJ shape variation and to classify the data. The number of resulting shape variables (p) varies between 1575 and 2646, depending of tooth position. The output data were imported in R with the package RToolsForDeformetrica v.0.1 (43). Using the packages ade4 v.1.7-6 (44) and Morpho v.2.8 (45) for R v.4.0.4 (46), we first computed principal component analyses (PCA), followed by between-group principal component analyses (bgPCA) using all PCs based on the deformation moments and using the following three groups assigned with equal prior probabilities: Early-Middle Pleistocene *Homo*,

Australopithecus and *Paranthropus*. The southern African purported *Homo* specimens were then projected a posteriori into the bgPCA morphospace. We followed the recommendations of Cardini and Polly (47) by computing the cross-validated bgPCA (cv-bgPCA) to assess the validity of the standard bgPCA group discrimination using the package Morpho v.2.8 (45). Our results show that the bgPCA and cv-bgPCA discriminate the three groups in a similar way (Figs. 2-3; *SI Appendix*, Figs. S9-S10). Statistical results show that for cv-bgPCA, R^2 ranges between 0.50 and 0.72 depending on tooth position and $p < 0.001$ for all tooth positions. The R^2 coefficient is thus far above zero (even if potentially inflated by small sample size), indicating that group separation is unlikely to be spurious (47). We also performed cross-validated canonical variates analyses (CVA) using the same groups as for the bgPCA using the R package Morpho v.2.8 (45). Since CVA computation requires the number of variables to be much smaller than the number of specimens, we computed the CVA based on a subset of the first PC scores (5-13) showing the highest degree of correct classification (screening the correct classification results and selecting the minimum number of PC scores enabling to reach the optimum of correct classification) (48). This choice of the PC scores subset is a compromise between including a sufficient proportion of overall shape variation and limiting the number of variables to avoid unrealistic and unstable levels of discrimination (49). We also assessed the structure of data and results, notably to test whether group separation in the analyses is not spurious (47). The amount of variance (R^2) explained by group differences in the raw shape data was estimated by computing a permutational analysis of variance (ANOVA; 1,000 permutations) based on the Euclidean distance between the means (40, 47) and implementing a Holm correction for multiple pairwise tests using the vegan v.2.5-7 (50) and pairwiseAdonis v.0.3 (51) packages. The results show statistical distinction of the three groups in the full shape space for all tooth positions but for M³s (*SI Appendix*, Table S3). Correct classification for each group and overall classification resulting from the cv-bgPCA and cross-validated CVA are reported in the *SI Appendix* Table S4. Altogether, bgPCA, cv-bgPCA and CVA analyses are consistent with each other and confirm that the groups observed in the bgPCA are unlikely to be spurious (52). Classification of the specimens was done using distances to the means and check for outliers relative to the most likely group was conducted for both CVA and bgPCA (the latter was computed using a multivariate normal model).

Allometry was tested using permutational multivariate analysis of covariance (MANCOVA; 10,000 permutations) (53) in which the explanatory variables are the EDJ area and the groups (genera), and the dependent variables are the PC scores (*SI Appendix*, Table S5).

Geochemical analysis of three specimens were conducted in this study (KB 5223 from Kromdraai, and SK 96 and SKX 268 from Swartkrans; SAHRA permit IDs 2538 and 2539). The three fossil teeth were sectioned with a high-precision diamond saw and polished to 10 μm smoothness. Laser-ablation combined with inductively coupled plasma-mass spectrometry (LA-ICP-MS) was used for trace elemental mapping analyses of the samples according to the previously published protocol (54, 55). The GARG ESI NW213 instrument coupled to an Agilent 7700 ICP-MS system set at Southern Cross University were used to map the samples by rastered laser beam along the tooth surface in a straight line. The laser spot size was 40

μm , laser scan speed of 80 $\mu\text{m}\cdot\text{s}^{-1}$, laser intensity of 80%, and an ICP-MS total integration time of 0.50 s produced data points that corresponded to a pixel size of approximately $40\times40 \mu\text{m}$. Certified standard reference materials (NIST610, NIST612 and NIST614) were used to assess signal drift and absolute concentrations. Elemental maps were constructed using the R Shiny application “shinyImaging” (56) (<http://labs.icahn.mssm.edu/lautenberglab>). The app transforms individual laser line csv files for each isotope into counts per second (cps) matrix (number of ablation lines multiplied by the number of ablation spots per ablation line). For each element, the gas blank collected during the first 10s of each laser lines was subtracted from the RasterStack and elements were normalized to ^{43}Ca . Background around the teeth (signal arising from the encasing resin or air) was converted to white coloration (no intensity) to increase clarity of the figures by isolating the dental tissue from its surroundings. Color scales were applied using the linear blue-red Lookup Table.

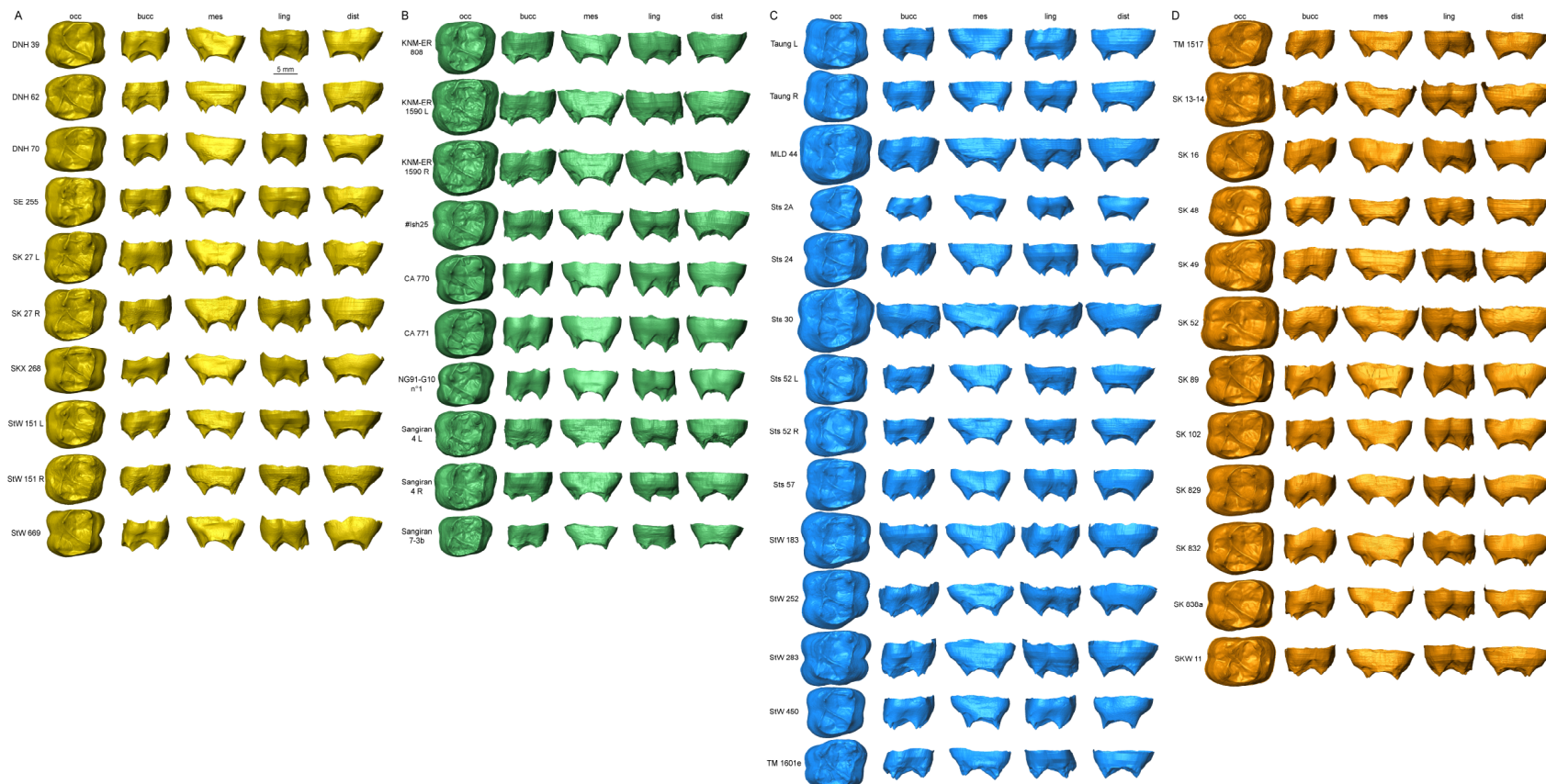


Fig. S1. The M¹ EDJ of the purported early *Homo* specimens from southern Africa (A) compared with those of Early to Middle Pleistocene *Homo* (B), *Australopithecus* (C) and *Paranthropus* (D).

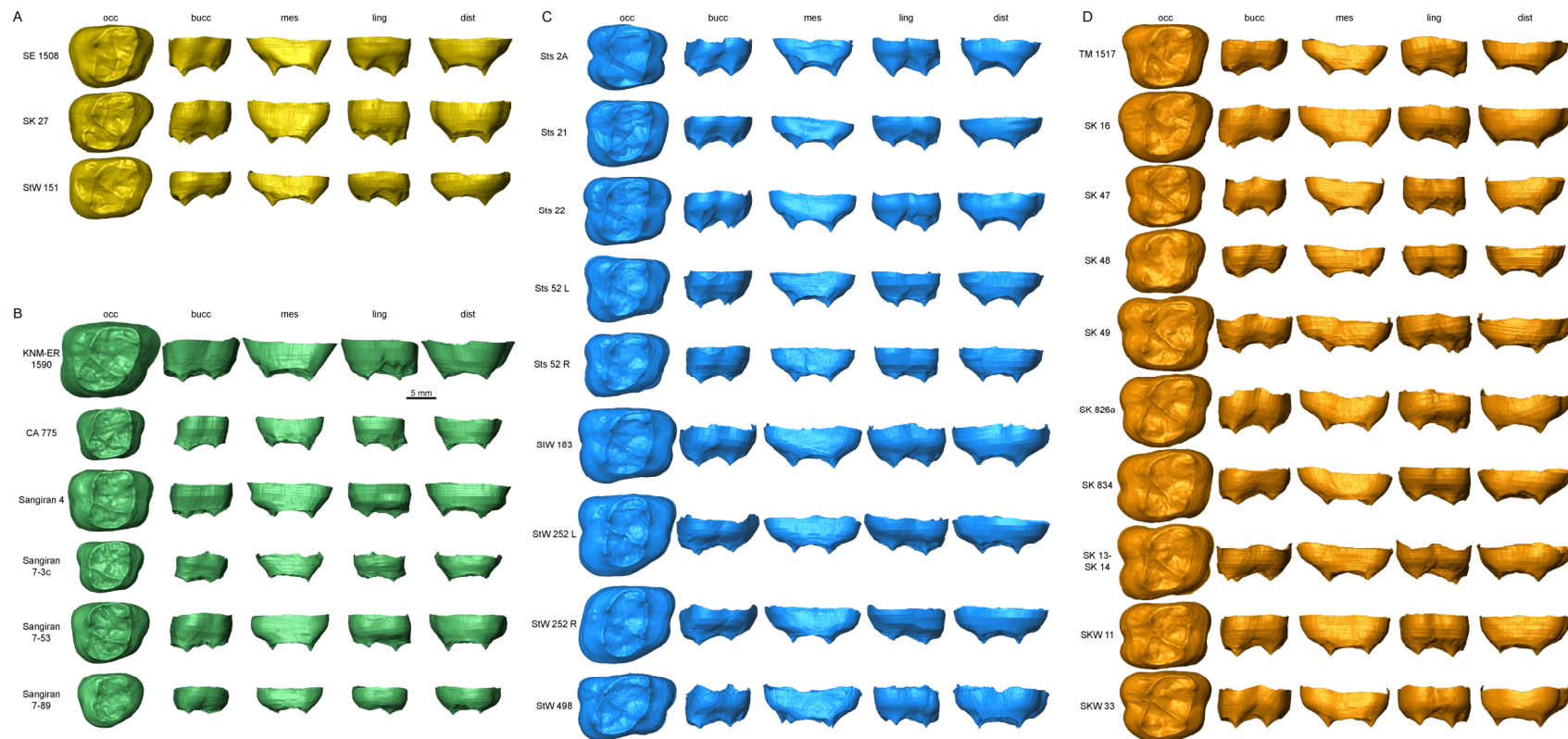


Fig. S2. The M² EDJ of the purported early *Homo* specimens from southern Africa (A) compared with those of Early to Middle Pleistocene *Homo* (B), *Australopithecus* (C) and *Paranthropus* (D).

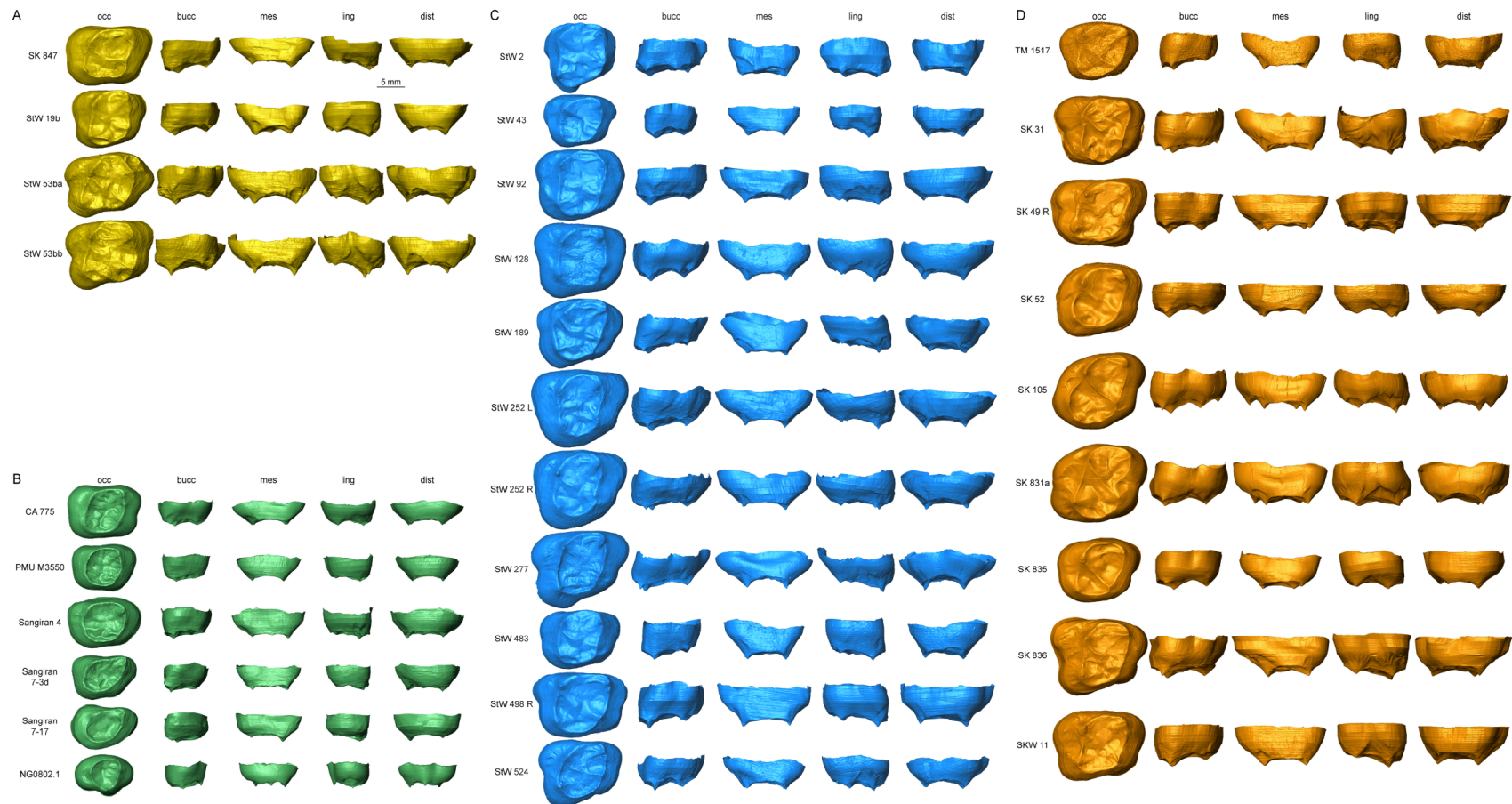


Fig. S3. The M^3 EDJ of the purported early *Homo* specimens from southern Africa (A) compared with those of Early to Middle Pleistocene *Homo* (B), *Australopithecus* (C) and *Paranthropus* (D).

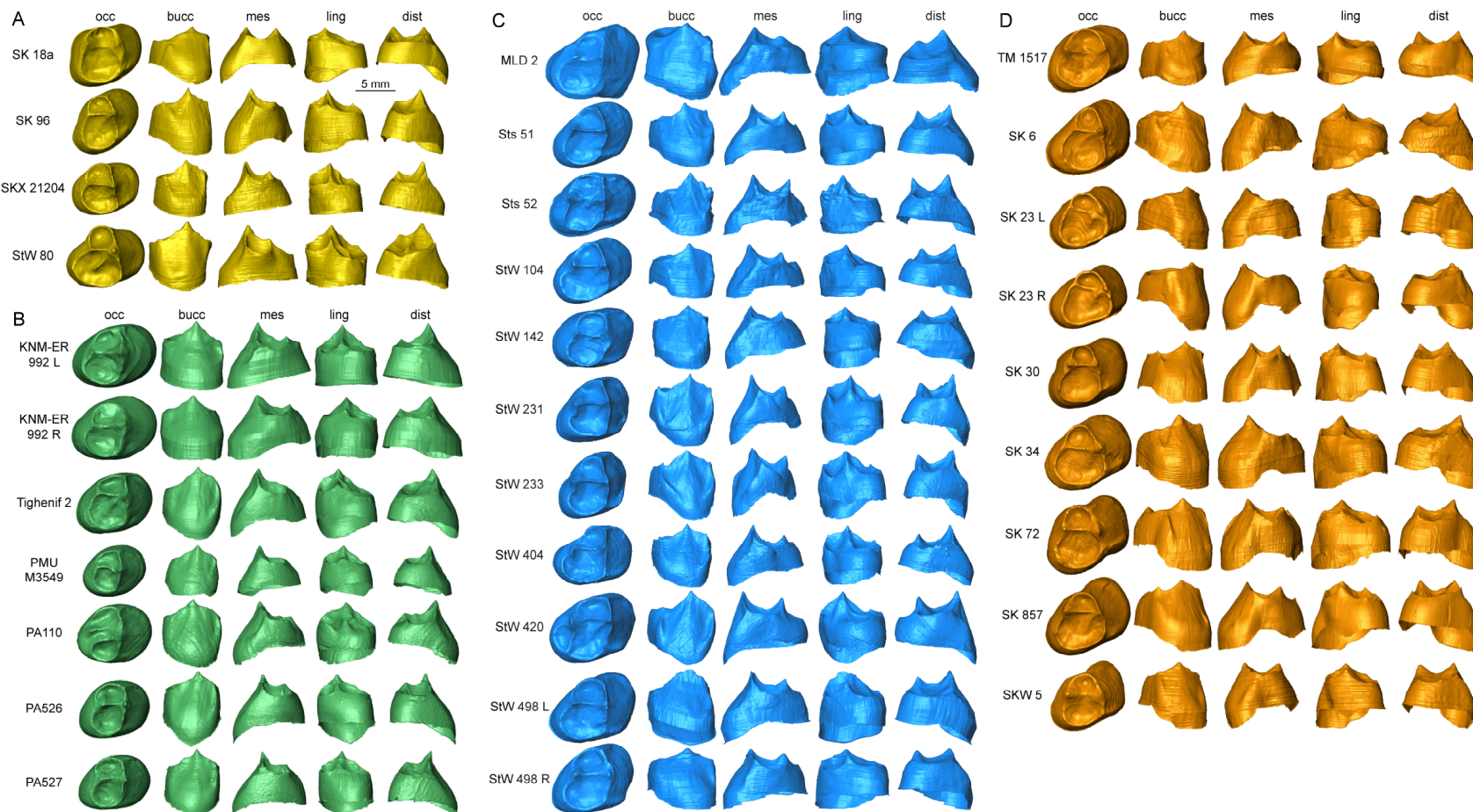


Fig. S4. The P₃ EDJ of the purported early *Homo* specimens from southern Africa (A) compared with those of Early to Middle Pleistocene *Homo* (B), *Australopithecus* (C) and *Paranthropus* (D).

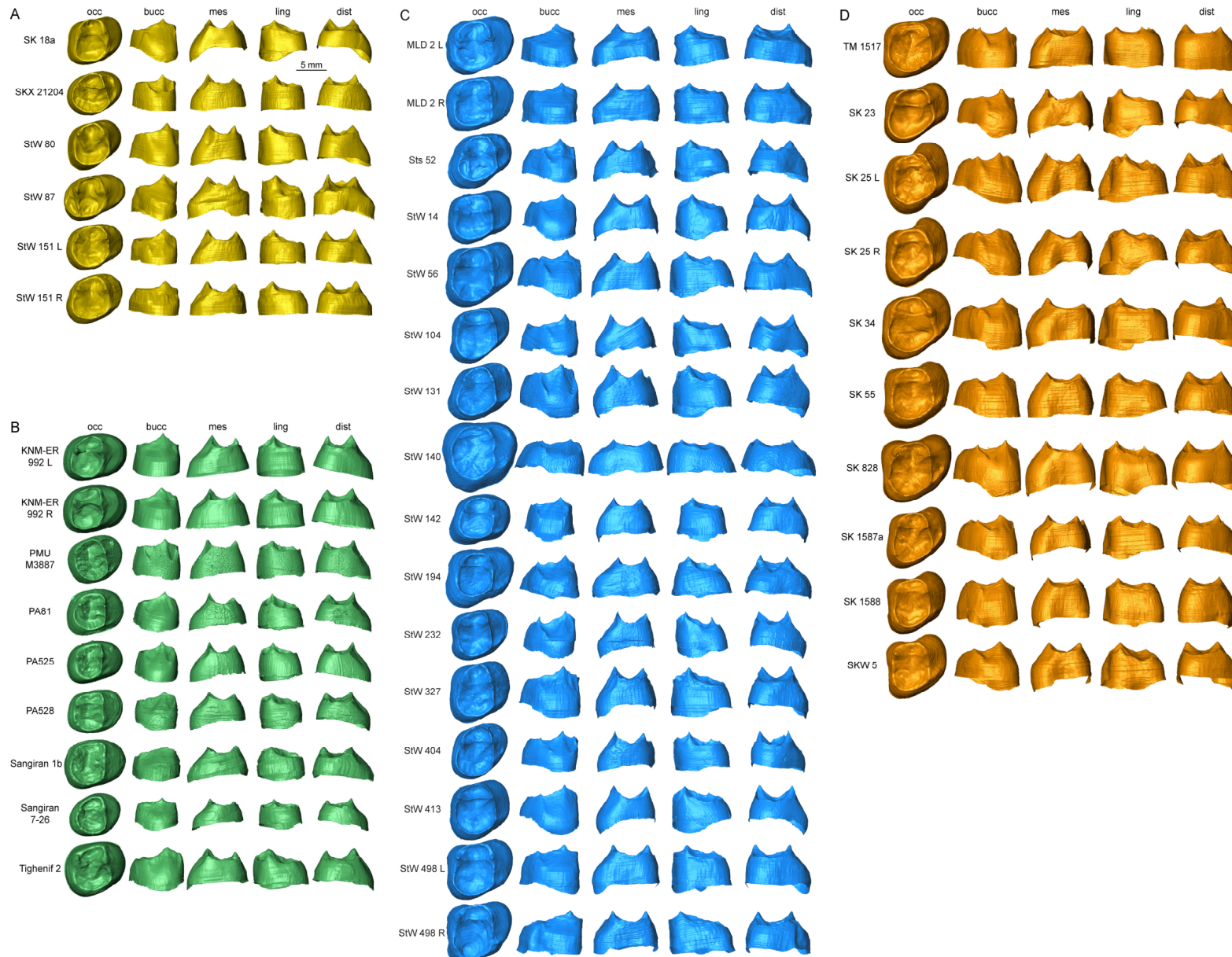


Fig. S5. The P₄ EDJ of the purported early *Homo* specimens from southern Africa (A) compared with those of Early to Middle Pleistocene *Homo* (B), *Australopithecus* (C) and *Paranthropus* (D).

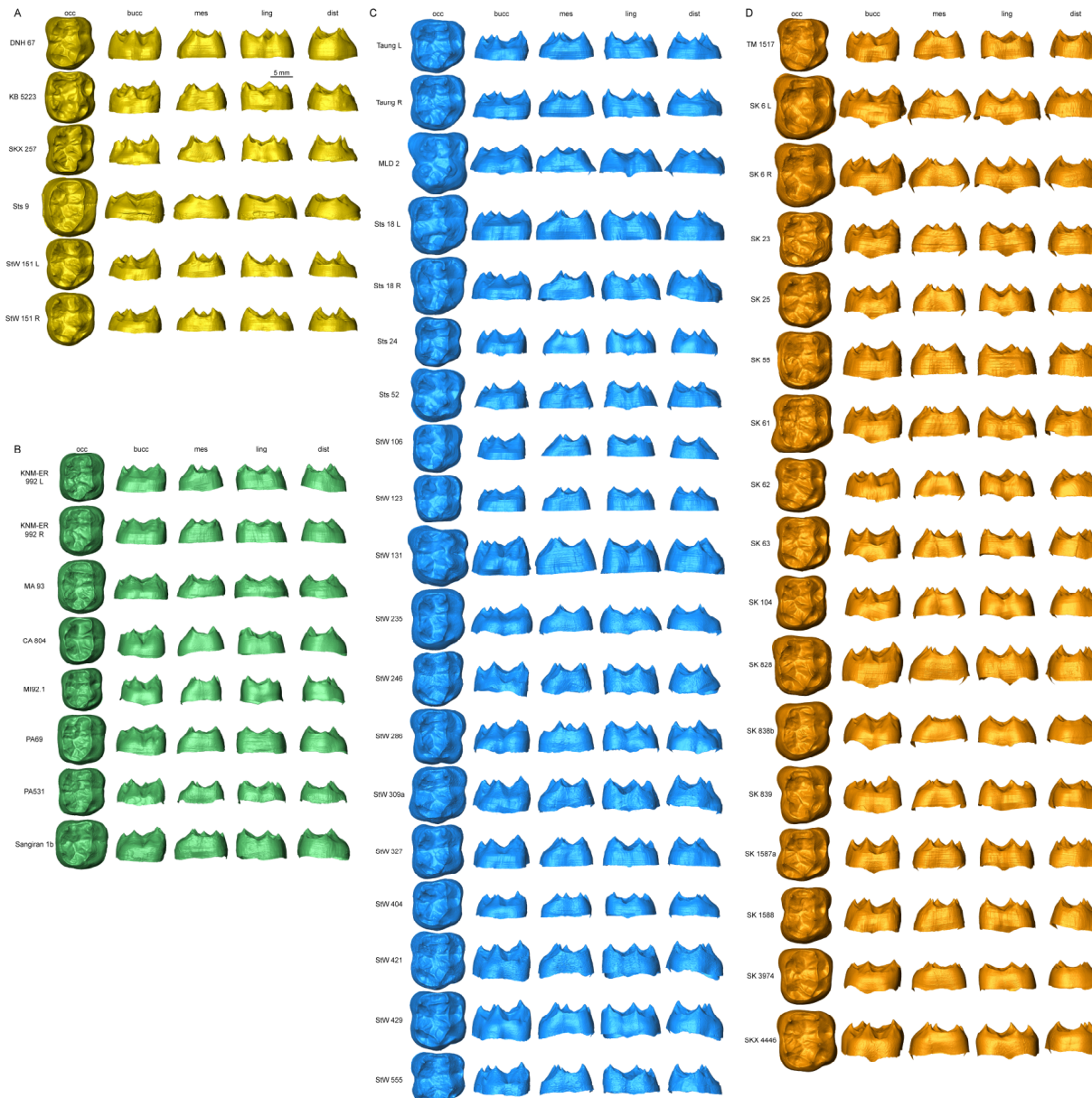


Fig. S6. The M₁ EDJ of the purported early *Homo* specimens from southern Africa (A) compared with those of Early to Middle Pleistocene *Homo* (B), *Australopithecus* (C) and *Paranthropus* (D).

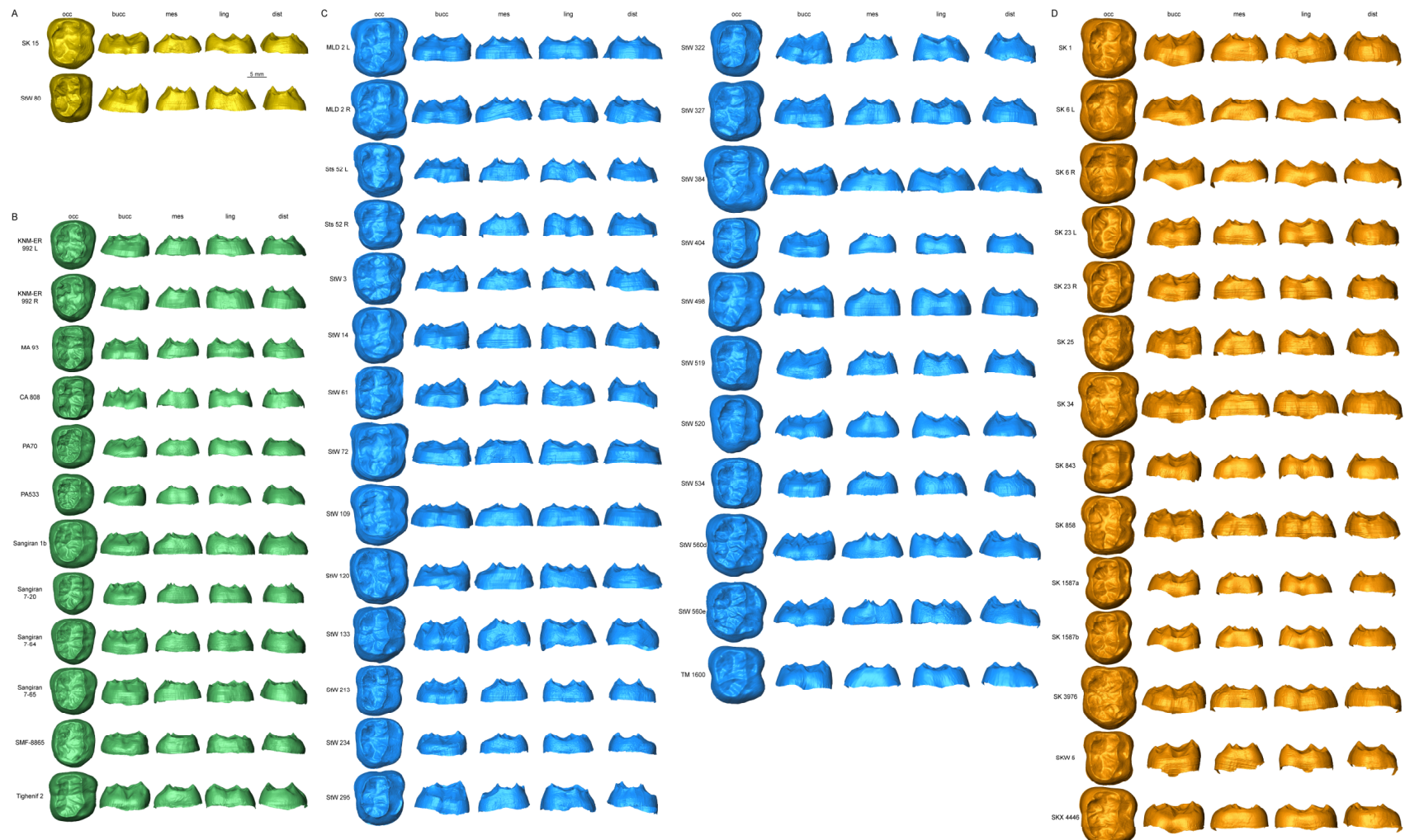


Fig. S7. The M₂ EDJ of the purported early *Homo* specimens from southern Africa (A) compared with those of Early to Middle Pleistocene *Homo* (B), *Australopithecus* (C) and *Paranthropus* (D).

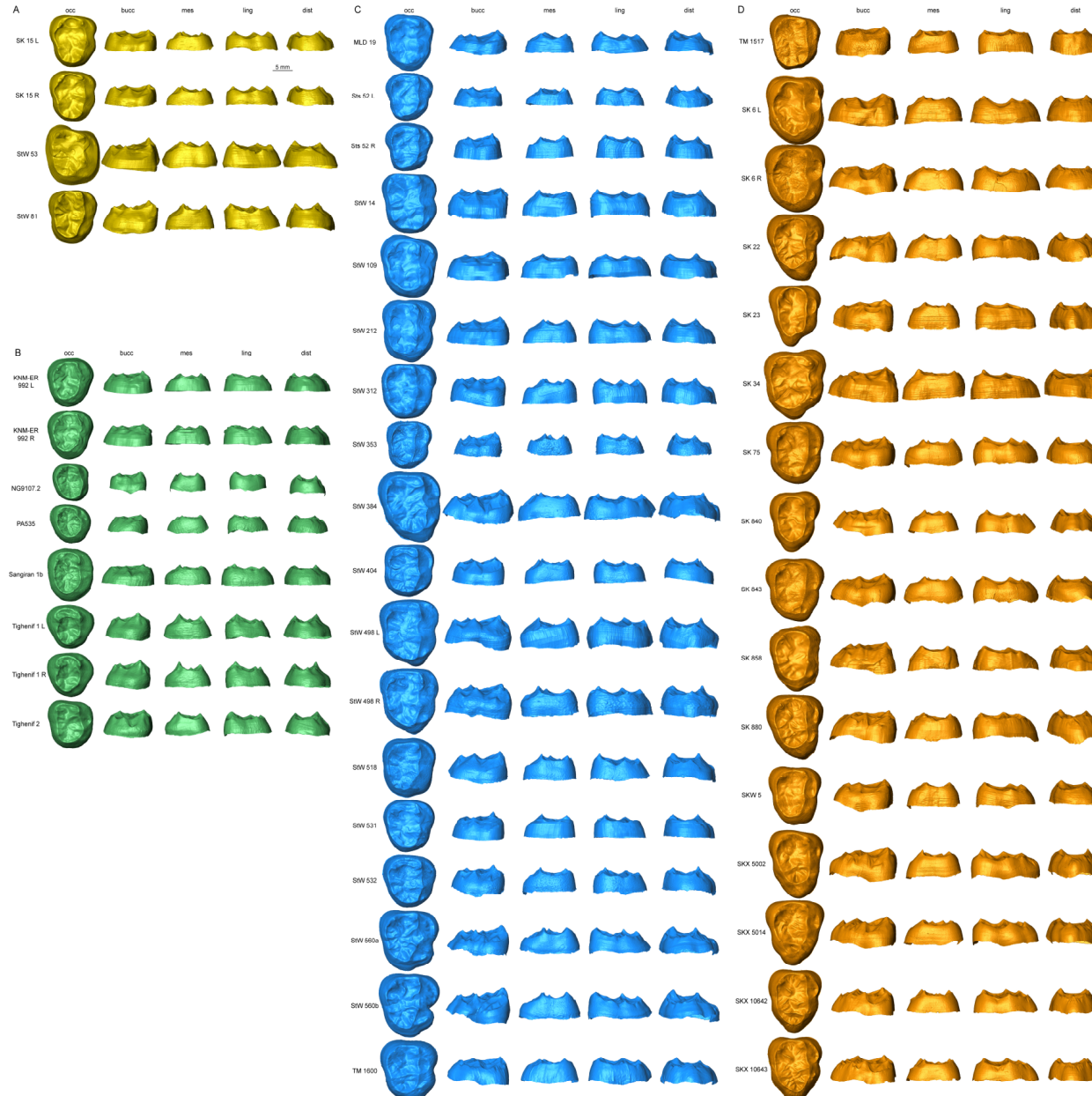


Fig. S8. The M₃ EDJ of the purported early *Homo* specimens from southern Africa (A) compared with those of Early to Middle Pleistocene *Homo* (B), *Australopithecus* (C) and *Paranthropus* (D).

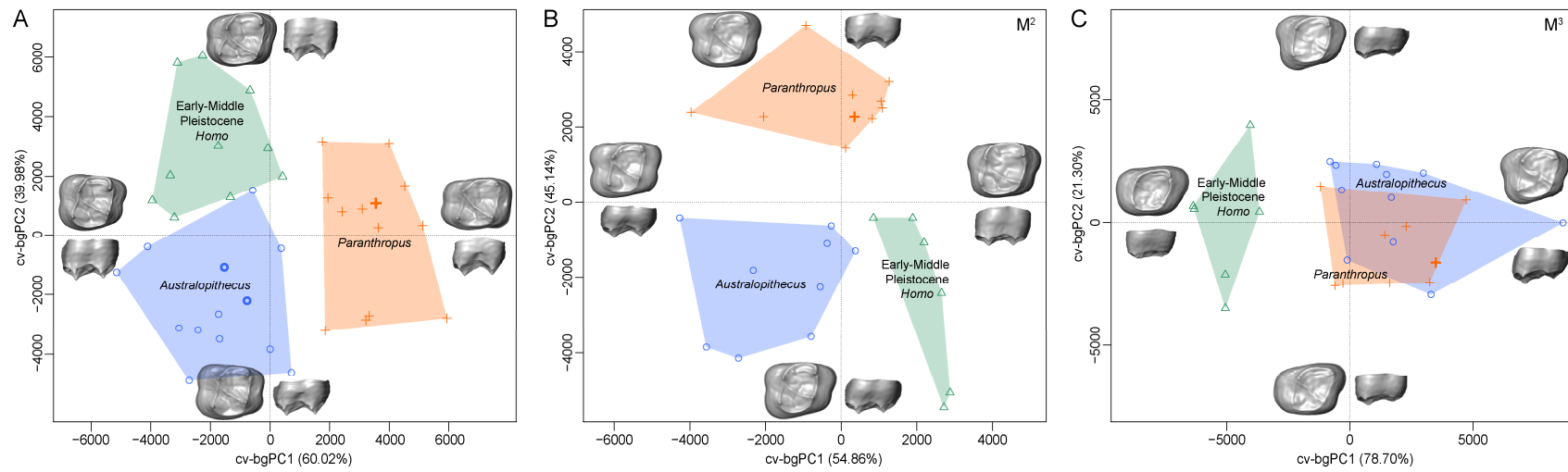


Fig. S9. Bivariate plot of the cross-validated between-group principal component analysis (cv-bgPCA) scores based on the dense surface matching (DSM) deformation fields for the M¹ (A), M² (B) and M³ (C). Symbols highlighted in bold represent the holotype specimens of *Australopithecus* (Taung) and *Paranthropus* (TM 1517).

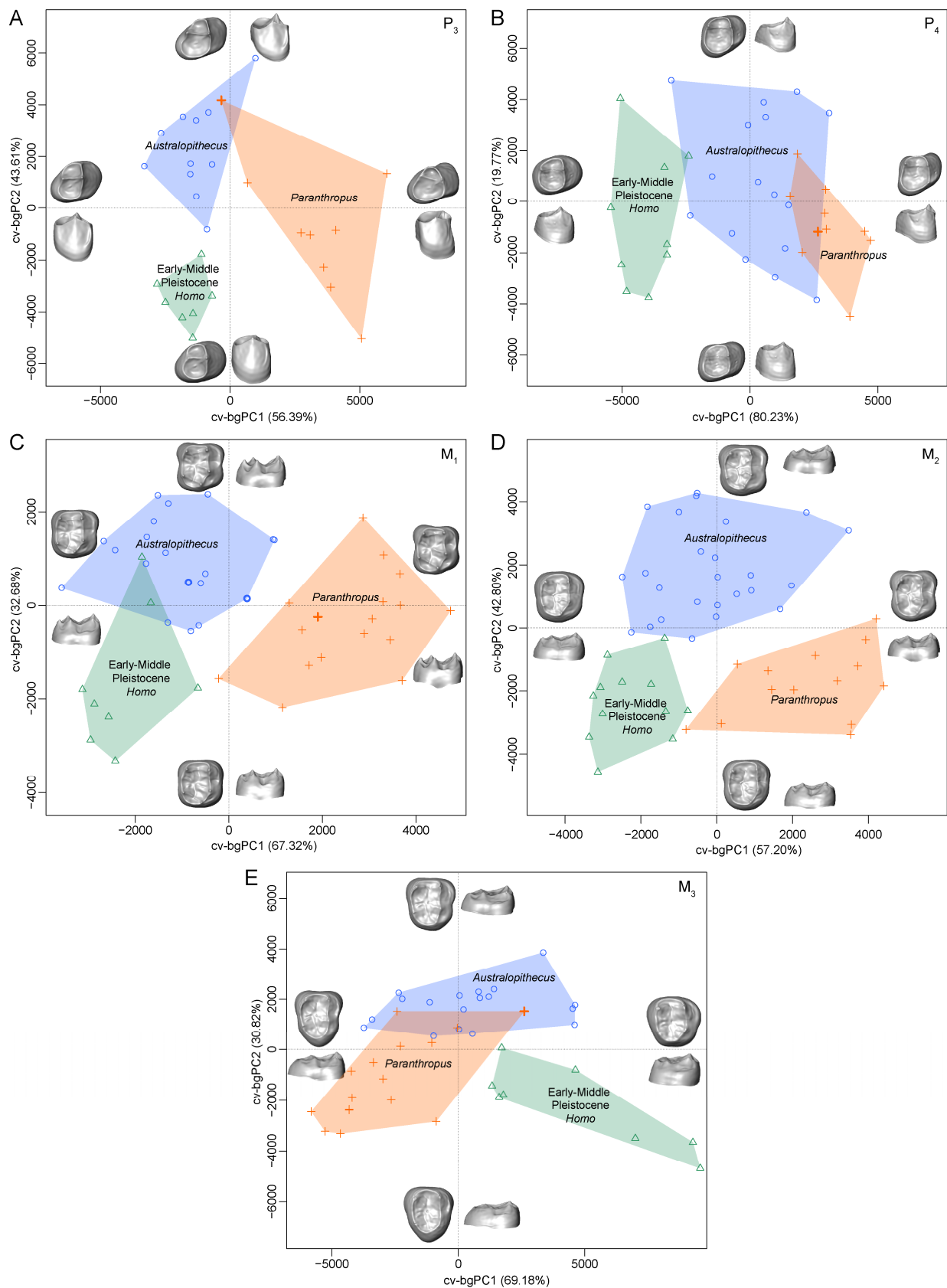


Fig. S10. Bivariate plot of the cross-validated between-group principal component analysis (cv-bgPCA) scores based on the dense surface matching (DSM) deformation fields for the P_3 (A), P_4 (B), M_1 (C), M_2 (D) and M_3 (E). Symbols highlighted in bold represent the holotype specimens of *Australopithecus* (Taung) and *Paranthropus* (TM 1517).

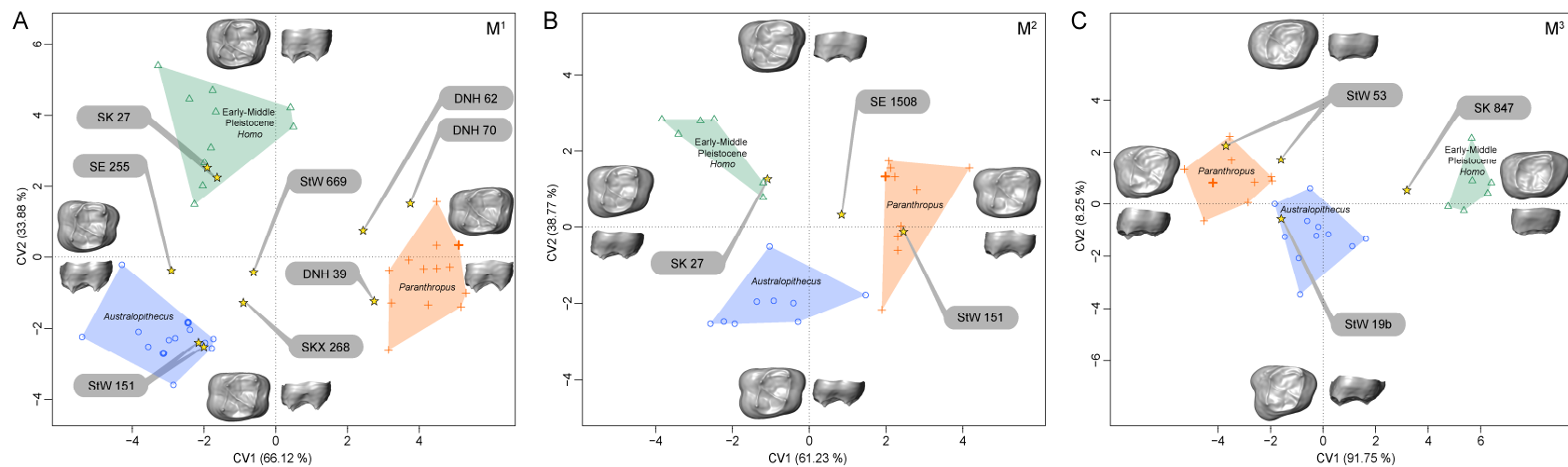


Fig. S11. Bivariate plot of the canonical variate analysis (CVA) scores based on subsets of PC scores for the M¹ (A), M² (B) and M³ (c). Symbols highlighted in bold represent the holotype specimens of *Australopithecus* (Taung) and *Paranthropus* (TM 1517).

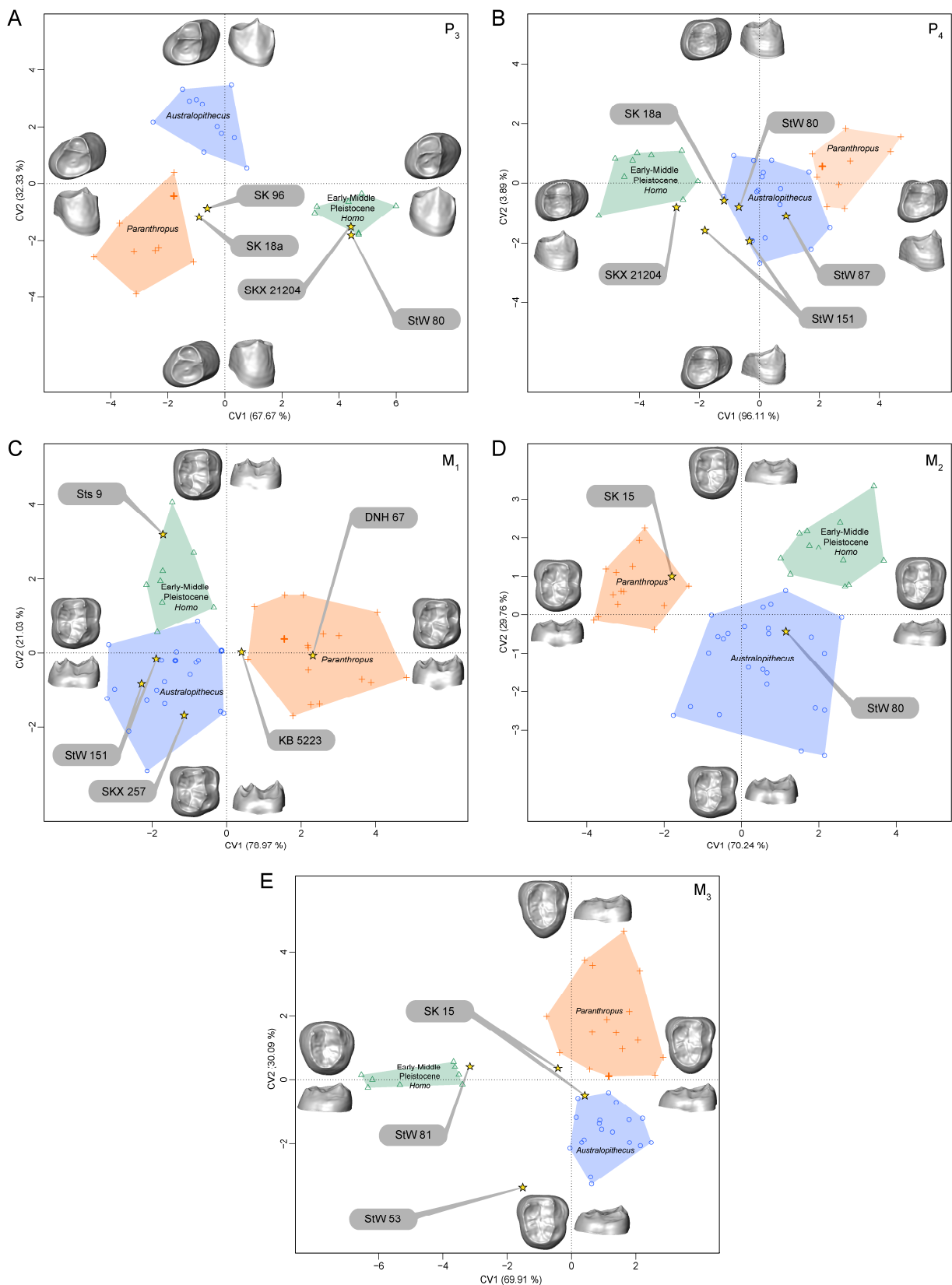


Fig. S12. Bivariate plot of the canonical variate analysis (CVA) scores based on subsets of PC scores for the P_3 (A), P_4 (B), M_1 (C), M_2 (D) and M_3 (E). Symbols highlighted in bold represent the holotype specimens of *Australopithecus* (Taung) and *Paranthropus* (TM 1517).

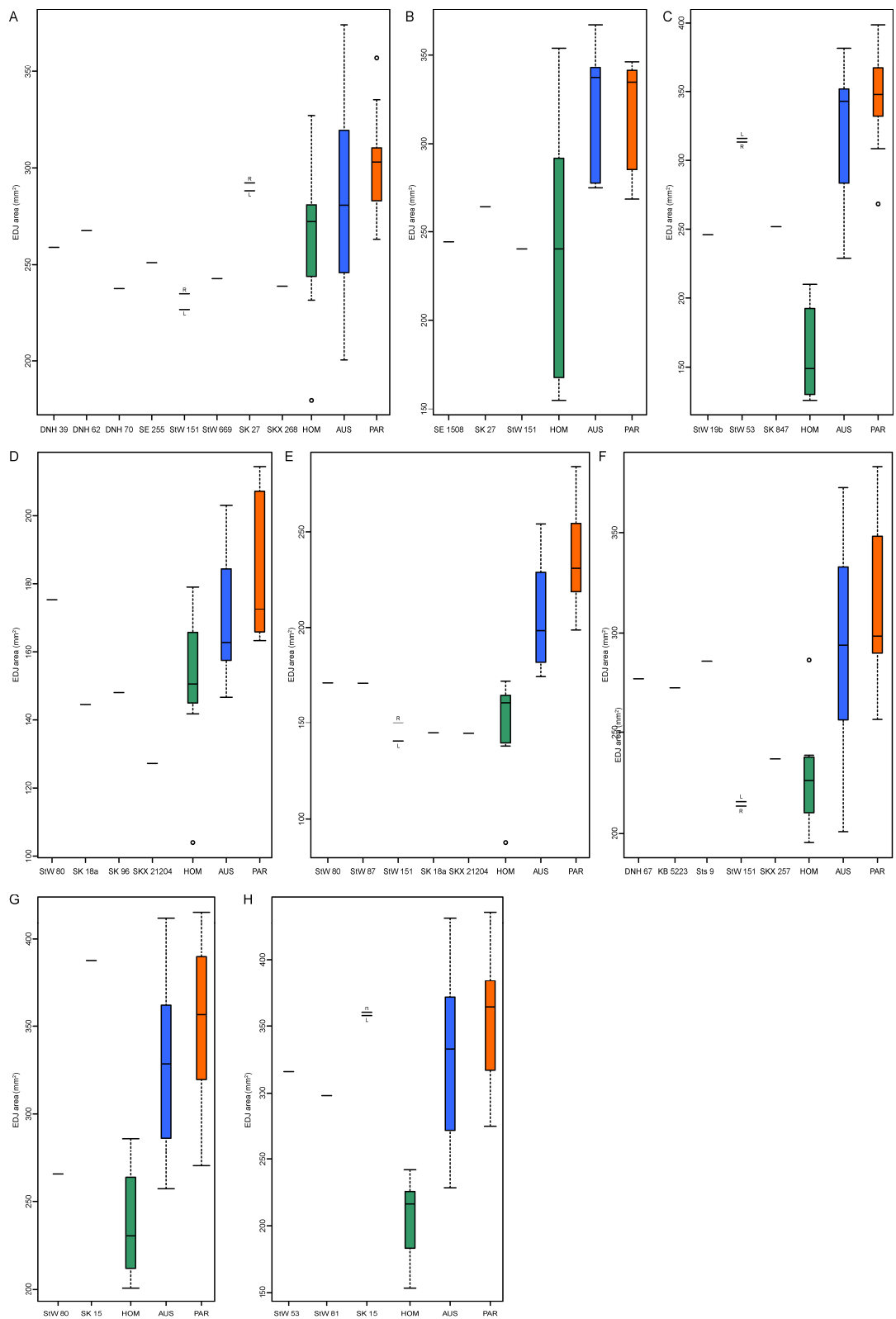


Fig. S13. Box and whisker plots of the EDJ area (used as a proxy for tooth size) of the purported southern African M¹ (A), M² (B), M³ (C), P₃ (D), P₄ (E), M₁ (F), M₂ (G) and M₃ (H) compared with those of Early to Middle Pleistocene *Homo* (HOM), *Australopithecus* (AUS) and *Paranthropus* (PAR). The boxplots show the median, the 25th and 75th percentiles (upper and lower hinges), and the range (lower and upper whiskers).

Table S1. List of the investigated southern African specimens previously attributed to *Homo* (with the exception of Sts 9 that was recognized as *Homo* in this study).

| specimen | tooth | site | stratigraphy | description | attribution to <i>Homo</i> |
|--------------|--|----------------|-------------------------------|-------------|----------------------------|
| DNH 39 | RM ¹ | Drimolen | Main Quarry | 12 | 12 |
| DNH 62 | LM ¹ | Drimolen | Main Quarry | 12 | 12 |
| DNH 67 | RM ₁ | Drimolen | Main Quarry | 12 | 12 |
| DNH 70 | LM ¹ | Drimolen | Main Quarry | 12 | 11 |
| KB 5223 | LM ₁ | Kromdraai B | Member 3/2? | 57 | 57 |
| SE 255 | RM ¹ | Sterkfontein | Member 5 (Extension Site) | 2, 58 | 16 |
| SE 1508 | RM ² | Sterkfontein | Member 5 (Extension Site) | 2, 58 | 16 |
| StW 19b | RM ³ | Sterkfontein | Member 4/5? | 13 | 7 |
| StW 53 | LM ³ , RM ³ , LM ₃ | Sterkfontein | Member 4/5? (StW 53 Infill) | 6 | 59 |
| StW 80 | RP ₃ , RP ₄ , RM ₂ | Sterkfontein | Member 5 (West) | 17 | 17 |
| StW 81 | RM ₃ | Sterkfontein | Member 5 (West) | 17 | 17 |
| StW 87 | RP ₄ | Sterkfontein | Member 4? | 13 | 7 |
| StW 151 | LM ¹ , RM ¹ , RM ² , LP ₄ , RP ₄ , LM ₁ , RM ₁ | Sterkfontein | Member 4 | 60 | 60 |
| StW 669 | RM ¹ | Sterkfontein | Millner Hall (STK-MH1 T1) | 18 | 18, 19 |
| Sts 9 | RM ₁ | Sterkfontein | Member 4/5? (Type Site) | 61 | this study |
| SK 15 | RM ₂ , LM ₃ , RM ₃ | Swartkrans | Member 2 | 1 | 1 |
| SK 18a | LP ₃ or LP ₄ | Swartkrans | Member 2 | 3 | 3 |
| SK 27 | LM ¹ , RM ¹ , RM ² | Swartkrans | Member 1 (Hanging Remnant) | 5 | 5 |
| SK 96 | LP ₃ | Swartkrans | Member 1 (Hanging Remnant) | 61 | 9 |
| SK 847 | LM ³ | Swartkrans | Member 1 (Hanging Remnant) | 6 | 6 |
| SKX 257 | RM ₁ | Swartkrans | Member 2 | 4 | 4 |
| SKX 268 | RM ¹ | Swartkrans | Member 2 | 4 | 4 |
| SKX 21204 | RP ₃ , RP ₄ | Swartkrans | Member 1 (Lower Bank) | 4 | 4 |

Table S2. List of the comparative microtomographic (microCT) data of dental remains attributed to *Australopithecus* (AUS), Early and Middle Pleistocene *Homo* (HOM), and *Paranthropus* (PAR).

| specimen | tooth | site | taxonomic attribution | Chronology | ref. of microCT data |
|---------------|----------------|-----------------------------|-----------------------|--------------------------|----------------------|
| MLD 44 | M ¹ | Makapansgat (South Africa) | AUS | Late Pliocene | this study |
| Sts 2A | M ¹ | Sterkfontein (South Africa) | AUS | ~2.8-2.2 Ma | this study |
| Sts 24 | M ¹ | Sterkfontein (South Africa) | AUS | ~2.8-2.2 Ma | this study |
| Sts 30 | M ¹ | Sterkfontein (South Africa) | AUS | ~2.8-2.2 Ma | this study |
| Sts 52 L | M ¹ | Sterkfontein (South Africa) | AUS | ~2.8-2.2 Ma | this study |
| Sts 52 R | M ¹ | Sterkfontein (South Africa) | AUS | ~2.8-2.2 Ma | this study |
| Sts 57 | M ¹ | Sterkfontein (South Africa) | AUS | ~2.8-2.2 Ma | this study |
| StW 252 | M ¹ | Sterkfontein (South Africa) | AUS | ~2.8-2.2 Ma | this study |
| StW 183 | M ¹ | Sterkfontein (South Africa) | AUS | ~2.8-2.2 Ma | this study |
| StW 283 | M ¹ | Sterkfontein (South Africa) | AUS | ~2.8-2.2 Ma | this study |
| StW 450 | M ¹ | Sterkfontein (South Africa) | AUS | ~2.8-2.2 Ma | this study |
| Taung L | M ¹ | Taung (South Africa) | AUS | Late Pliocene | this study |
| Taung R | M ¹ | Taung (South Africa) | AUS | Late Pliocene | this study |
| TM 1601e | M ¹ | Sterkfontein (South Africa) | AUS | ~2.8-2.2 Ma | this study |
| CA 770 | M ¹ | China | HOM | Middle Pleistocene | 62 |
| CA 771 | M ¹ | China | HOM | Middle Pleistocene | 62 |
| #Ish25 | M ¹ | Ishango (D.R. Congo) | HOM | Early Pleistocene | 63 |
| KNM-ER 808 | M ¹ | Koobi Fora (Kenya) | HOM | ~1.5 Ma | this study |
| KNM-ER 1590 L | M ¹ | Koobi Fora (Kenya) | HOM | ~1.5-1.4 Ma | 64 |
| KNM-ER 1590 R | M ¹ | Koobi Fora (Kenya) | HOM | ~1.5-1.4 Ma | 64 |
| NG91-G10 n°1 | M ¹ | Ngebung (Indonesia) | HOM | early Middle Pleistocene | 22 |
| Sangiran 4 L | M ¹ | Sangiran (Indonesia) | HOM | Early Pleistocene | 39, 65 |
| Sangiran 4 R | M ¹ | Sangiran (Indonesia) | HOM | Early Pleistocene | 39, 65 |
| Sangiran 7-3b | M ¹ | Sangiran (Indonesia) | HOM | Early Pleistocene | this study |
| SK 13-14 | M ¹ | Swartkrans (South Africa) | PAR | ~2.2-1.8 Ma | this study |
| SK 16 | M ¹ | Swartkrans (South Africa) | PAR | ~2.2-1.8 Ma | this study |
| SK 48 | M ¹ | Swartkrans (South Africa) | PAR | ~2.2-1.8 Ma | this study |

| | | | | | |
|---------------|----------------|-----------------------------|-----|---------------------------|------------|
| SK 49 | M ¹ | Swartkrans (South Africa) | PAR | ~2.2-1.8 Ma | this study |
| SK 52 | M ¹ | Swartkrans (South Africa) | PAR | ~2.2-1.8 Ma | this study |
| SK 89 | M ¹ | Swartkrans (South Africa) | PAR | ~2.2-1.8 Ma | this study |
| SK 102 | M ¹ | Swartkrans (South Africa) | PAR | ~2.2-1.8 Ma | this study |
| SK 829 | M ¹ | Swartkrans (South Africa) | PAR | ~2.2-1.8 Ma | this study |
| SK 832 | M ¹ | Swartkrans (South Africa) | PAR | ~2.2-1.8 Ma | this study |
| SK 838a | M ¹ | Swartkrans (South Africa) | PAR | ~2.2-1.8 Ma | this study |
| SKW 11 | M ¹ | Swartkrans (South Africa) | PAR | ~2.2-1.8 Ma | this study |
| TM 1517 | M ¹ | Kromdraai (South Africa) | PAR | initial Early Pleistocene | this study |
| Sts 2A | M ² | Sterkfontein (South Africa) | AUS | ~2.8-2.2 Ma | this study |
| Sts 21 | M ² | Sterkfontein (South Africa) | AUS | ~2.8-2.2 Ma | this study |
| Sts 22 | M ² | Sterkfontein (South Africa) | AUS | ~2.8-2.2 Ma | this study |
| Sts 52 L | M ² | Sterkfontein (South Africa) | AUS | ~2.8-2.2 Ma | this study |
| Sts 52 R | M ² | Sterkfontein (South Africa) | AUS | ~2.8-2.2 Ma | this study |
| StW 183 | M ² | Sterkfontein (South Africa) | AUS | ~2.8-2.2 Ma | this study |
| StW 252 L | M ² | Sterkfontein (South Africa) | AUS | ~2.8-2.2 Ma | this study |
| StW 252 R | M ² | Sterkfontein (South Africa) | AUS | ~2.8-2.2 Ma | this study |
| StW 498 | M ² | Sterkfontein (South Africa) | AUS | ~2.8-2.2 Ma | this study |
| CA 775 | M ² | China | HOM | Middle Pleistocene | 62 |
| KNM-ER 1590M | M ² | Koobi Fora (Kenya) | HOM | ~1.5-1.4 Ma | 64 |
| Sangiran 4 | M ² | Sangiran (Indonesia) | HOM | Early Pleistocene | 39, 65 |
| Sangiran 7-3c | M ² | Sangiran (Indonesia) | HOM | Early Pleistocene | this study |
| Sangiran 7-53 | M ² | Sangiran (Indonesia) | HOM | Early Pleistocene | this study |
| Sangiran 7-89 | M ² | Sangiran (Indonesia) | HOM | Early Pleistocene | this study |
| SK 13-14 | M ² | Swartkrans (South Africa) | PAR | ~2.2-1.8 Ma | this study |
| SK 16 | M ² | Swartkrans (South Africa) | PAR | ~2.2-1.8 Ma | this study |
| SK 47 | M ² | Swartkrans (South Africa) | PAR | ~2.2-1.8 Ma | this study |
| SK 48 | M ² | Swartkrans (South Africa) | PAR | ~2.2-1.8 Ma | this study |
| SK 49 | M ² | Swartkrans (South Africa) | PAR | ~2.2-1.8 Ma | this study |
| SK 826a2 | M ² | Swartkrans (South Africa) | PAR | ~2.2-1.8 Ma | this study |

| | | | | | |
|---------------|----------------|-----------------------------|-----|---------------------------|------------|
| SK 834 | M ² | Swartkrans (South Africa) | PAR | ~2.2-1.8 Ma | this study |
| SKW 11 | M ² | Swartkrans (South Africa) | PAR | ~2.2-1.8 Ma | this study |
| SKW 33-14129 | M ² | Swartkrans (South Africa) | PAR | ~2.2-1.8 Ma | this study |
| TM 1517 | M ² | Kromdraai (South Africa) | PAR | initial Early Pleistocene | this study |
| StW 2 | M ³ | Sterkfontein (South Africa) | AUS | ~2.8-2.2 Ma | this study |
| StW 43 | M ³ | Sterkfontein (South Africa) | AUS | ~2.8-2.2 Ma | this study |
| StW 92 | M ³ | Sterkfontein (South Africa) | AUS | ~2.8-2.2 Ma | this study |
| StW 128 | M ³ | Sterkfontein (South Africa) | AUS | ~2.8-2.2 Ma | this study |
| StW 189 | M ³ | Sterkfontein (South Africa) | AUS | ~2.8-2.2 Ma | this study |
| StW 252 L | M ³ | Sterkfontein (South Africa) | AUS | ~2.8-2.2 Ma | this study |
| StW 252 R | M ³ | Sterkfontein (South Africa) | AUS | ~2.8-2.2 Ma | this study |
| StW 277 | M ³ | Sterkfontein (South Africa) | AUS | ~2.8-2.2 Ma | this study |
| StW 483 | M ³ | Sterkfontein (South Africa) | AUS | ~2.8-2.2 Ma | this study |
| StW 498 | M ³ | Sterkfontein (South Africa) | AUS | ~2.8-2.2 Ma | this study |
| StW 524 | M ³ | Sterkfontein (South Africa) | AUS | ~2.8-2.2 Ma | this study |
| CA 772 | M ³ | China | HOM | Middle Pleistocene | 62 |
| M3550 | M ³ | Zhoukoudian (China) | HOM | ~0.8-0.7 Ma | 39, 65 |
| NG0802.1 | M ³ | Ngebung (Indonesia) | HOM | Middle Pleistocene | 22 |
| Sangiran 4 | M ³ | Sangiran (Indonesia) | HOM | Early Pleistocene | 39, 65 |
| Sangiran 7-3d | M ³ | Sangiran (Indonesia) | HOM | Early Pleistocene | this study |
| Sangiran 7-17 | M ³ | Sangiran (Indonesia) | HOM | Early Pleistocene | this study |
| SK 31 | M ³ | Swartkrans (South Africa) | PAR | ~2.2-1.8 Ma | this study |
| SK 49 | M ³ | Swartkrans (South Africa) | PAR | ~2.2-1.8 Ma | this study |
| SK 52 | M ³ | Swartkrans (South Africa) | PAR | ~2.2-1.8 Ma | this study |
| SK 105 | M ³ | Swartkrans (South Africa) | PAR | ~2.2-1.8 Ma | this study |
| SK 831a | M ³ | Swartkrans (South Africa) | PAR | ~2.2-1.8 Ma | this study |
| SK 835 | M ³ | Swartkrans (South Africa) | PAR | ~2.2-1.8 Ma | this study |
| SK 836 | M ³ | Swartkrans (South Africa) | PAR | ~2.2-1.8 Ma | this study |
| SKW 11 | M ³ | Swartkrans (South Africa) | PAR | ~2.2-1.8 Ma | this study |
| TM 1517 | M ³ | Kromdraai (South Africa) | PAR | initial Early Pleistocene | this study |

| | | | | | |
|--------------|----------------|-----------------------------|-----|---------------------------|------------|
| MLD 2 | P ₃ | Makapansgat (South Africa) | AUS | Late Pliocene | this study |
| Sts 51 | P ₃ | Sterkfontein (South Africa) | AUS | ~2.8-2.2 Ma | this study |
| Sts 52 | P ₃ | Sterkfontein (South Africa) | AUS | ~2.8-2.2 Ma | this study |
| StW 104 | P ₃ | Sterkfontein (South Africa) | AUS | ~2.8-2.2 Ma | this study |
| StW 142 | P ₃ | Sterkfontein (South Africa) | AUS | ~2.8-2.2 Ma | this study |
| StW 231 | P ₃ | Sterkfontein (South Africa) | AUS | ~2.8-2.2 Ma | this study |
| StW 233 | P ₃ | Sterkfontein (South Africa) | AUS | ~2.8-2.2 Ma | this study |
| StW 404 | P ₃ | Sterkfontein (South Africa) | AUS | ~2.8-2.2 Ma | this study |
| StW 420 | P ₃ | Sterkfontein (South Africa) | AUS | ~2.8-2.2 Ma | this study |
| StW 498 L | P ₃ | Sterkfontein (South Africa) | AUS | ~2.8-2.2 Ma | this study |
| StW 498 R | P ₃ | Sterkfontein (South Africa) | AUS | ~2.8-2.2 Ma | this study |
| KNM-ER 992 L | P ₃ | Koobi Fora (Kenya) | HOM | ~1.5 Ma | this study |
| KNM-ER 992 R | P ₃ | Koobi Fora (Kenya) | HOM | ~1.5 Ma | this study |
| M3549 | P ₃ | Zhoukoudian (China) | HOM | ~0.8-0.7 Ma | 39 |
| PA110 | P ₃ | Zhoukoudian (China) | HOM | ~0.5-0.3 Ma | 42, 66 67 |
| PA526 | P ₃ | Xichuan (China) | HOM | Middle Pleistocene | 42, 66 67 |
| PA527 | P ₃ | Xichuan (China) | HOM | Middle Pleistocene | 42, 66 |
| Tighenif 2 | P ₃ | Tighenif (Algeria) | HOM | ~1.0 Ma | 68 |
| SK 6 | P ₃ | Swartkrans (South Africa) | PAR | ~2.2-1.8 Ma | this study |
| SK 23 L | P ₃ | Swartkrans (South Africa) | PAR | ~2.2-1.8 Ma | this study |
| SK 23 R | P ₃ | Swartkrans (South Africa) | PAR | ~2.2-1.8 Ma | this study |
| SK 30 | P ₃ | Swartkrans (South Africa) | PAR | ~2.2-1.8 Ma | this study |
| SK 34 | P ₃ | Swartkrans (South Africa) | PAR | ~2.2-1.8 Ma | this study |
| SK 72 | P ₃ | Swartkrans (South Africa) | PAR | ~2.2-1.8 Ma | this study |
| SK 857 | P ₃ | Swartkrans (South Africa) | PAR | ~2.2-1.8 Ma | this study |
| SKW 5 | P ₃ | Swartkrans (South Africa) | PAR | ~2.2-1.8 Ma | this study |
| TM 1517 | P ₃ | Kromdraai (South Africa) | PAR | initial Early Pleistocene | this study |
| MLD 2 L | P ₄ | Makapansgat (South Africa) | AUS | Late Pliocene | this study |
| MLD 2 R | P ₄ | Makapansgat (South Africa) | AUS | Late Pliocene | this study |
| Sts 52 | P ₄ | Sterkfontein (South Africa) | AUS | ~2.8-2.2 Ma | this study |

| | | | | | |
|---------------|----------------|-----------------------------|-----|--------------------|------------|
| StW 14 | P ₄ | Sterkfontein (South Africa) | AUS | ~2.8-2.2 Ma | this study |
| StW 56 | P ₄ | Sterkfontein (South Africa) | AUS | ~2.8-2.2 Ma | this study |
| StW 104 | P ₄ | Sterkfontein (South Africa) | AUS | ~2.8-2.2 Ma | this study |
| StW 131 | P ₄ | Sterkfontein (South Africa) | AUS | ~2.8-2.2 Ma | this study |
| StW 140 | P ₄ | Sterkfontein (South Africa) | AUS | ~2.8-2.2 Ma | this study |
| StW 142 | P ₄ | Sterkfontein (South Africa) | AUS | ~2.8-2.2 Ma | this study |
| StW 194 | P ₄ | Sterkfontein (South Africa) | AUS | ~2.8-2.2 Ma | this study |
| StW 232 | P ₄ | Sterkfontein (South Africa) | AUS | ~2.8-2.2 Ma | this study |
| StW 327 | P ₄ | Sterkfontein (South Africa) | AUS | ~2.8-2.2 Ma | this study |
| StW 404 | P ₄ | Sterkfontein (South Africa) | AUS | ~2.8-2.2 Ma | this study |
| StW 413 | P ₄ | Sterkfontein (South Africa) | AUS | ~2.8-2.2 Ma | this study |
| StW 498 L | P ₄ | Sterkfontein (South Africa) | AUS | ~2.8-2.2 Ma | this study |
| StW 498 R | P ₄ | Sterkfontein (South Africa) | AUS | ~2.8-2.2 Ma | this study |
| KNM-ER 992B L | P ₄ | Koobi Fora (Kenya) | HOM | ~1.5 Ma | this study |
| KNM-ER 992B R | P ₄ | Koobi Fora (Kenya) | HOM | ~1.5 Ma | this study |
| M3887 | P ₄ | Zhoukoudian (China) | HOM | ~0.8-0.7 Ma | 39, 65 |
| PA81 | P ₄ | Changyang (China) | HOM | ~0.2 Ma | 42, 66 67 |
| PA525 | P ₄ | Xichuan (China) | HOM | Middle Pleistocene | 42, 66 67 |
| PA528 | P ₄ | Xichuan (China) | HOM | Middle Pleistocene | 42 |
| Sangiran 1b | P ₄ | Sangiran (Indonesia) | HOM | Early Pleistocene | 65,69 |
| Sangiran 7-26 | P ₄ | Sangiran (Indonesia) | HOM | Early Pleistocene | this study |
| Tighenif 2 | P ₄ | Tighenif (Algeria) | HOM | ~1.0 Ma | 68 |
| SK 23 | P ₄ | Swartkrans (South Africa) | PAR | ~2.2-1.8 Ma | this study |
| SK 25 L | P ₄ | Swartkrans (South Africa) | PAR | ~2.2-1.8 Ma | this study |
| SK 25 R | P ₄ | Swartkrans (South Africa) | PAR | ~2.2-1.8 Ma | this study |
| SK 34 L | P ₄ | Swartkrans (South Africa) | PAR | ~2.2-1.8 Ma | this study |
| SK 55 | P ₄ | Swartkrans (South Africa) | PAR | ~2.2-1.8 Ma | this study |
| SK 828 | P ₄ | Swartkrans (South Africa) | PAR | ~2.2-1.8 Ma | this study |
| SK 1587a | P ₄ | Swartkrans (South Africa) | PAR | ~2.2-1.8 Ma | this study |
| SK 1588 | P ₄ | Swartkrans (South Africa) | PAR | ~2.2-1.8 Ma | this study |

| | | | | | |
|--------------|----------------|-----------------------------|-----|---------------------------|------------|
| SKW 5 | P ₄ | Swartkrans (South Africa) | PAR | ~2.2-1.8 Ma | this study |
| TM 1517 | P ₄ | Kromdraai (South Africa) | PAR | initial Early Pleistocene | this study |
| MLD 2 | M ₁ | Makapansgat (South Africa) | AUS | Late Pliocene | this study |
| Sts 18 L | M ₁ | Sterkfontein (South Africa) | AUS | ~2.8-2.2 Ma | this study |
| Sts 18 R | M ₁ | Sterkfontein (South Africa) | AUS | ~2.8-2.2 Ma | this study |
| Sts 24 | M ₁ | Sterkfontein (South Africa) | AUS | ~2.8-2.2 Ma | this study |
| Sts 52 | M ₁ | Sterkfontein (South Africa) | AUS | ~2.8-2.2 Ma | this study |
| StW 106 | M ₁ | Sterkfontein (South Africa) | AUS | ~2.8-2.2 Ma | this study |
| StW 123 | M ₁ | Sterkfontein (South Africa) | AUS | ~2.8-2.2 Ma | this study |
| StW 131 | M ₁ | Sterkfontein (South Africa) | AUS | ~2.8-2.2 Ma | this study |
| StW 235 | M ₁ | Sterkfontein (South Africa) | AUS | ~2.8-2.2 Ma | this study |
| StW 246 | M ₁ | Sterkfontein (South Africa) | AUS | ~2.8-2.2 Ma | this study |
| StW 286 | M ₁ | Sterkfontein (South Africa) | AUS | ~2.8-2.2 Ma | this study |
| StW 309a | M ₁ | Sterkfontein (South Africa) | AUS | ~2.8-2.2 Ma | this study |
| StW 327 | M ₁ | Sterkfontein (South Africa) | AUS | ~2.8-2.2 Ma | this study |
| StW 404 | M ₁ | Sterkfontein (South Africa) | AUS | ~2.8-2.2 Ma | this study |
| StW 421 | M ₁ | Sterkfontein (South Africa) | AUS | ~2.8-2.2 Ma | this study |
| StW 429 | M ₁ | Sterkfontein (South Africa) | AUS | ~2.8-2.2 Ma | this study |
| StW 555 | M ₁ | Sterkfontein (South Africa) | AUS | ~2.8-2.2 Ma | this study |
| Taung L | M ₁ | Taung (South Africa) | AUS | Late Pliocene | this study |
| Taung R | M ₁ | Taung (South Africa) | AUS | Late Pliocene | this study |
| CA 804 | M ₁ | China | HOM | Middle Pleistocene | 62 |
| KNM-ER 992 L | M ₁ | Koobi Fora (Kenya) | HOM | ~1.5 Ma | 70 |
| KNM-ER 992 R | M ₁ | Koobi Fora (Kenya) | HOM | ~1.5 Ma | 70 |
| MA 93 | M ₁ | Mulhuli Amo (Eritrea) | HOM | ~1.0 Ma | 71 |
| MI92.1 | M ₁ | Miri (Indonesia) | HOM | Middle Pleistocene | 72 |
| PA69 | M ₁ | Zhoukoudian (China) | HOM | ~0.8-0.7 Ma | 73 |
| PA531 | M ₁ | Xichuan (China) | HOM | Middle Pleistocene | 73 |
| Sangiran 1b | M ₁ | Sangiran (Indonesia) | HOM | Early Pleistocene | 65, 69 |
| SK 6 L | M ₁ | Swartkrans (South Africa) | PAR | ~2.2-1.8 Ma | this study |

| | | | | | |
|----------|----------------|-----------------------------|-----|---------------------------|------------|
| SK 6 R | M ₁ | Swartkrans (South Africa) | PAR | ~2.2-1.8 Ma | this study |
| SK 23 | M ₁ | Swartkrans (South Africa) | PAR | ~2.2-1.8 Ma | this study |
| SK 25 | M ₁ | Swartkrans (South Africa) | PAR | ~2.2-1.8 Ma | this study |
| SK 55 | M ₁ | Swartkrans (South Africa) | PAR | ~2.2-1.8 Ma | this study |
| SK 61 | M ₁ | Swartkrans (South Africa) | PAR | ~2.2-1.8 Ma | this study |
| SK 62 | M ₁ | Swartkrans (South Africa) | PAR | ~2.2-1.8 Ma | this study |
| SK 63 | M ₁ | Swartkrans (South Africa) | PAR | ~2.2-1.8 Ma | this study |
| SK 104 | M ₁ | Swartkrans (South Africa) | PAR | ~2.2-1.8 Ma | this study |
| SK 828 | M ₁ | Swartkrans (South Africa) | PAR | ~2.2-1.8 Ma | this study |
| SK 838b | M ₁ | Swartkrans (South Africa) | PAR | ~2.2-1.8 Ma | this study |
| SK 839 | M ₁ | Swartkrans (South Africa) | PAR | ~2.2-1.8 Ma | this study |
| SK 1587a | M ₁ | Swartkrans (South Africa) | PAR | ~2.2-1.8 Ma | this study |
| SK 1588 | M ₁ | Swartkrans (South Africa) | PAR | ~2.2-1.8 Ma | this study |
| SK 3974 | M ₁ | Swartkrans (South Africa) | PAR | ~2.2-1.8 Ma | this study |
| SKX 4446 | M ₁ | Swartkrans (South Africa) | PAR | ~1.4 Ma | this study |
| TM 1517 | M ₁ | Kromdraai (South Africa) | PAR | initial Early Pleistocene | this study |
| MLD 2 L | M ₂ | Makapansgat (South Africa) | AUS | Late Pliocene | this study |
| MLD 2 R | M ₂ | Makapansgat (South Africa) | AUS | Late Pliocene | this study |
| Sts 52 L | M ₂ | Sterkfontein (South Africa) | AUS | ~2.8-2.2 Ma | this study |
| Sts 52 R | M ₂ | Sterkfontein (South Africa) | AUS | ~2.8-2.2 Ma | this study |
| StW 3 | M ₂ | Sterkfontein (South Africa) | AUS | ~2.8-2.2 Ma | this study |
| StW 14 | M ₂ | Sterkfontein (South Africa) | AUS | ~2.8-2.2 Ma | this study |
| StW 61 | M ₂ | Sterkfontein (South Africa) | AUS | ~2.8-2.2 Ma | this study |
| StW 72 | M ₂ | Sterkfontein (South Africa) | AUS | ~2.8-2.2 Ma | this study |
| StW 109 | M ₂ | Sterkfontein (South Africa) | AUS | ~2.8-2.2 Ma | this study |
| StW 120 | M ₂ | Sterkfontein (South Africa) | AUS | ~2.8-2.2 Ma | this study |
| StW 133 | M ₂ | Sterkfontein (South Africa) | AUS | ~2.8-2.2 Ma | this study |
| StW 213 | M ₂ | Sterkfontein (South Africa) | AUS | ~2.8-2.2 Ma | this study |
| StW 234 | M ₂ | Sterkfontein (South Africa) | AUS | ~2.8-2.2 Ma | this study |
| StW 295 | M ₂ | Sterkfontein (South Africa) | AUS | ~2.8-2.2 Ma | this study |

| | | | | | |
|---------------|----------------|-----------------------------|-----|--------------------|------------|
| StW 322 | M ₂ | Sterkfontein (South Africa) | AUS | ~2.8-2.2 Ma | this study |
| StW 327 | M ₂ | Sterkfontein (South Africa) | AUS | ~2.8-2.2 Ma | this study |
| StW 384 | M ₂ | Sterkfontein (South Africa) | AUS | ~2.8-2.2 Ma | this study |
| StW 404 | M ₂ | Sterkfontein (South Africa) | AUS | ~2.8-2.2 Ma | this study |
| StW 498 | M ₂ | Sterkfontein (South Africa) | AUS | ~2.8-2.2 Ma | this study |
| StW 519 | M ₂ | Sterkfontein (South Africa) | AUS | ~2.8-2.2 Ma | this study |
| StW 520 | M ₂ | Sterkfontein (South Africa) | AUS | ~2.8-2.2 Ma | this study |
| StW 534 | M ₂ | Sterkfontein (South Africa) | AUS | ~2.8-2.2 Ma | this study |
| StW 560d | M ₂ | Sterkfontein (South Africa) | AUS | ~2.8-2.2 Ma | this study |
| StW 560e | M ₂ | Sterkfontein (South Africa) | AUS | ~2.8-2.2 Ma | this study |
| TM 1600 | M ₂ | Sterkfontein (South Africa) | AUS | ~2.8-2.2 Ma | this study |
| CA 808 | M ₂ | China | HOM | Middle Pleistocene | 62 |
| KNM-ER 992 L | M ₂ | Koobi Fora (Kenya) | HOM | ~1.5 Ma | 70 |
| KNM-ER 992 R | M ₂ | Koobi Fora (Kenya) | HOM | ~1.5 Ma | 70 |
| MA 93 | M ₂ | Mulhuli Amo (Eritrea) | HOM | ~1.0 Ma | 71 |
| PA70 | M ₂ | Zhoukoudian (China) | HOM | ~0.8-0.7 Ma | 73 |
| PA533 | M ₂ | Xichuan (China) | HOM | Middle Pleistocene | this study |
| Sangiran 1b | M ₂ | Sangiran (Indonesia) | HOM | Early Pleistocene | 65, 69 |
| Sangiran 7-20 | M ₂ | Sangiran (Indonesia) | HOM | Early Pleistocene | 27 |
| Sangiran 7-64 | M ₂ | Sangiran (Indonesia) | HOM | Early Pleistocene | this study |
| Sangiran 7-65 | M ₂ | Sangiran (Indonesia) | HOM | Early Pleistocene | 27 |
| SMF-8865 | M ₂ | Sangiran (Indonesia) | HOM | Early Pleistocene | 65 |
| Tighenif 2 | M ₂ | Tighenif (Algeria) | HOM | ~1.0 Ma | 68 |
| SK 1 | M ₂ | Swartkrans (South Africa) | PAR | ~2.2-1.8 Ma | this study |
| SK 6 L | M ₂ | Swartkrans (South Africa) | PAR | ~2.2-1.8 Ma | this study |
| SK 6 R | M ₂ | Swartkrans (South Africa) | PAR | ~2.2-1.8 Ma | this study |
| SK 23 L | M ₂ | Swartkrans (South Africa) | PAR | ~2.2-1.8 Ma | this study |
| SK 23 R | M ₂ | Swartkrans (South Africa) | PAR | ~2.2-1.8 Ma | this study |
| SK 25 L | M ₂ | Swartkrans (South Africa) | PAR | ~2.2-1.8 Ma | this study |
| SK 34 R | M ₂ | Swartkrans (South Africa) | PAR | ~2.2-1.8 Ma | this study |

| | | | | | |
|--------------|----------------|-----------------------------|-----|--------------------|------------|
| SK 843 | M ₂ | Swartkrans (South Africa) | PAR | ~2.2-1.8 Ma | this study |
| SK 858 R | M ₂ | Swartkrans (South Africa) | PAR | ~2.2-1.8 Ma | this study |
| SK 1587a | M ₂ | Swartkrans (South Africa) | PAR | ~2.2-1.8 Ma | this study |
| SK 1587b | M ₂ | Swartkrans (South Africa) | PAR | ~2.2-1.8 Ma | this study |
| SK 3976 | M ₂ | Swartkrans (South Africa) | PAR | ~2.2-1.8 Ma | this study |
| SKW 5 L | M ₂ | Swartkrans (South Africa) | PAR | ~2.2-1.8 Ma | this study |
| SKX 4446 | M ₂ | Swartkrans (South Africa) | PAR | ~2.2-1.8 Ma | this study |
| MLD 19 | M ₃ | Makapansgat (South Africa) | AUS | Late Pliocene | this study |
| Sts 52 L | M ₃ | Sterkfontein (South Africa) | AUS | ~2.8-2.2 Ma | this study |
| Sts 52 R | M ₃ | Sterkfontein (South Africa) | AUS | ~2.8-2.2 Ma | this study |
| StW 14 | M ₃ | Sterkfontein (South Africa) | AUS | ~2.8-2.2 Ma | this study |
| StW 109 | M ₃ | Sterkfontein (South Africa) | AUS | ~2.8-2.2 Ma | this study |
| StW 212 | M ₃ | Sterkfontein (South Africa) | AUS | ~2.8-2.2 Ma | this study |
| StW 312 | M ₃ | Sterkfontein (South Africa) | AUS | ~2.8-2.2 Ma | this study |
| StW 353 | M ₃ | Sterkfontein (South Africa) | AUS | ~2.8-2.2 Ma | this study |
| StW 384 | M ₃ | Sterkfontein (South Africa) | AUS | ~2.8-2.2 Ma | this study |
| StW 404 | M ₃ | Sterkfontein (South Africa) | AUS | ~2.8-2.2 Ma | this study |
| StW 498 L | M ₃ | Sterkfontein (South Africa) | AUS | ~2.8-2.2 Ma | this study |
| StW 498 R | M ₃ | Sterkfontein (South Africa) | AUS | ~2.8-2.2 Ma | this study |
| StW 518 | M ₃ | Sterkfontein (South Africa) | AUS | ~2.8-2.2 Ma | this study |
| StW 531 | M ₃ | Sterkfontein (South Africa) | AUS | ~2.8-2.2 Ma | this study |
| StW 532 | M ₃ | Sterkfontein (South Africa) | AUS | ~2.8-2.2 Ma | this study |
| StW 560a | M ₃ | Sterkfontein (South Africa) | AUS | ~2.8-2.2 Ma | this study |
| StW 560b | M ₃ | Sterkfontein (South Africa) | AUS | ~2.8-2.2 Ma | this study |
| TM1600 | M ₃ | Sterkfontein (South Africa) | AUS | ~2.8-2.2 Ma | this study |
| KNM-ER 992 L | M ₃ | Koobi Fora (Kenya) | HOM | ~1.5 Ma | 70 |
| KNM-ER 992 R | M ₃ | Koobi Fora (Kenya) | HOM | ~1.5 Ma | 70 |
| NG9107.2 | M ₃ | Ngebung (Indonesia) | HOM | Middle Pleistocene | 22 |
| PA535 | M ₃ | Xichuan (China) | HOM | Middle Pleistocene | this study |
| Sangiran 1b | M ₃ | Sangiran (Indonesia) | HOM | Early Pleistocene | 65, 69 |

| | | | | | |
|--------------|----------------|---------------------------|-----|---------------------------|------------|
| Tighenif 1 L | M ₃ | Tighenif (Algeria) | HOM | ~1.0 Ma | 68 |
| Tighenif 1 R | M ₃ | Tighenif (Algeria) | HOM | ~1.0 Ma | 68 |
| Tighenif 2 | M ₃ | Tighenif (Algeria) | HOM | ~1.0 Ma | 68 |
| SK 6 L | M ₃ | Swartkrans (South Africa) | PAR | ~2.2-1.8 Ma | this study |
| SK 6 R | M ₃ | Swartkrans (South Africa) | PAR | ~2.2-1.8 Ma | this study |
| SK 22 | M ₃ | Swartkrans (South Africa) | PAR | ~2.2-1.8 Ma | this study |
| SK 23 | M ₃ | Swartkrans (South Africa) | PAR | ~2.2-1.8 Ma | this study |
| SK 34 | M ₃ | Swartkrans (South Africa) | PAR | ~2.2-1.8 Ma | this study |
| SK 75 | M ₃ | Swartkrans (South Africa) | PAR | ~2.2-1.8 Ma | this study |
| SK 840 | M ₃ | Swartkrans (South Africa) | PAR | ~2.2-1.8 Ma | this study |
| SK 843 | M ₃ | Swartkrans (South Africa) | PAR | ~2.2-1.8 Ma | this study |
| SK 858 | M ₃ | Swartkrans (South Africa) | PAR | ~2.2-1.8 Ma | this study |
| SK 880 | M ₃ | Swartkrans (South Africa) | PAR | ~2.2-1.8 Ma | this study |
| SKW 5 | M ₃ | Swartkrans (South Africa) | PAR | ~2.2-1.8 Ma | this study |
| SKX 5002 | M ₃ | Swartkrans (South Africa) | PAR | ~2.2-1.8 Ma | this study |
| SKX 5014 | M ₃ | Swartkrans (South Africa) | PAR | ~2.2-1.8 Ma | this study |
| SKX 10642 | M ₃ | Swartkrans (South Africa) | PAR | ~2.2-1.8 Ma | this study |
| SKX 10643 | M ₃ | Swartkrans (South Africa) | PAR | ~2.2-1.8 Ma | this study |
| TM 1517 | M ₃ | Kromdraai (South Africa) | PAR | initial Early Pleistocene | this study |

Table S3. Results of the permutational ANOVA testing the group structure in the shape data. AUST: *Australopithecus*; HOM: Early and Middle Pleistocene *Homo*; PAR: *Paranthropus*. Significant values are highlighted in bold.

| tooth | groups compared | R ² | adjusted p-value |
|----------------|-----------------|----------------|------------------|
| M ¹ | AUST vs. HE | 0.17 | <0.01 |
| | AUST vs. PROB | 0.15 | <0.01 |
| | HE vs. PROB | 0.20 | <0.01 |
| M ² | AUST vs. HE | 0.20 | <0.01 |
| | AUST vs. PROB | 0.16 | <0.01 |
| | HE vs. PROB | 0.21 | <0.01 |
| M ³ | AUST vs. HE | 0.21 | <0.01 |
| | AUST vs. PROB | 0.07 | 0.11 |
| | HE vs. PROB | 0.24 | <0.01 |
| P ₃ | AUST vs. HE | 0.23 | <0.01 |
| | AUST vs. PROB | 0.23 | <0.01 |
| | HE vs. PROB | 0.31 | <0.01 |
| P ₄ | AUST vs. HE | 0.15 | <0.01 |
| | AUST vs. PROB | 0.10 | <0.01 |
| | HE vs. PROB | 0.33 | <0.01 |
| M ₁ | AUST vs. HE | 0.08 | 0.02 |
| | AUST vs. PROB | 0.11 | <0.01 |
| | HE vs. PROB | 0.17 | <0.01 |
| M ₂ | AUST vs. HE | 0.11 | <0.01 |
| | AUST vs. PROB | 0.11 | <0.01 |
| | HE vs. PROB | 0.21 | <0.01 |
| M ₃ | AUST vs. HE | 0.14 | <0.01 |
| | AUST vs. PROB | 0.11 | <0.01 |
| | HE vs. PROB | 0.22 | <0.01 |

Table S4. Cross-validated bgPCA and CVA proportions of correctly classified individuals using shape data and *Australopithecus* (AUS), Early and Middle Pleistocene *Homo* (HOM), and *Paranthropus* (PAR) used as a priori groups.

| | HOM | | AUS | | PAR | | overall accuracy | |
|----------------------|--------------|------------|--------------|------------|--------------|------------|------------------|-------------|
| M¹ | bgPCA: 10/10 | CVA: 10/10 | bgPCA: 12/13 | CVA: 13/13 | bgPCA: 13/13 | CVA: 13/13 | bgPCA: 97.2% | CVA: 100.0% |
| M² | bgPCA: 5/6 | CVA: 6/6 | bgPCA: 9/9 | CVA: 8/9 | bgPCA: 10/10 | CVA: 9/10 | bgPCA: 96.0% | CVA: 92.0% |
| M³ | bgPCA: 6/6 | CVA: 6/6 | bgPCA: 8/11 | CVA: 10/11 | bgPCA: 6/9 | CVA: 7/9 | bgPCA: 76.9% | CVA: 88.5% |
| P₃ | bgPCA: 7/7 | CVA: 7/7 | bgPCA: 10/11 | CVA: 11/11 | bgPCA: 7/9 | CVA: 7/9 | bgPCA: 88.9% | CVA: 92.6% |
| P₄ | bgPCA: 8/9 | CVA: 9/9 | bgPCA: 11/16 | CVA: 13/16 | bgPCA: 8/10 | CVA: 9/10 | bgPCA: 77.1% | CVA: 88.6% |
| M₁ | bgPCA: 6/8 | CVA: 7/8 | bgPCA: 19/19 | CVA: 18/19 | bgPCA: 16/17 | CVA: 16/17 | bgPCA: 93.2% | CVA: 93.2% |
| M₂ | bgPCA: 12/12 | CVA: 12/12 | bgPCA: 24/25 | CVA: 23/25 | bgPCA: 13/14 | CVA: 14/14 | bgPCA: 96.1% | CVA: 96.1% |
| M₃ | bgPCA: 6/8 | CVA: 8/8 | bgPCA: 15/18 | CVA: 18/18 | bgPCA: 12/16 | CVA: 13/16 | bgPCA: 78.6% | CVA: 92.9% |

Table S5. Results of permutational multivariate analysis of shape (all PC scores) covariance using EDJ area as covariate and genera as groups. Significant values are highlighted in bold.

| Tooth | Source of variation | Model with interaction (PCs~EDJ _{area} *groups) | | Model without size (PCs~groups) | |
|----------------------|---------------------|---|-----------------|------------------------------------|-----------------|
| | | R ² | p-value | R ² | p-value |
| M¹ | EDJ area | 0.05 | 0.02 | | |
| | groups (genera) | 0.22 | <0.01 | 0.22 | <0.01 |
| | interaction | 0.06 | 0.09 | | |
| M² | EDJ area | 0.09 | <0.01 | | |
| | groups (genera) | 0.19 | <0.01 | 0.25 | <0.01 |
| | interaction | 0.06 | 0.60 | | |
| M³ | EDJ area | 0.15 | <0.01 | | |
| | groups (genera) | 0.09 | 0.17 | 0.21 | <0.01 |
| | interaction | 0.09 | 0.13 | | |
| P₃ | EDJ area | 0.06 | 0.03 | | |
| | groups (genera) | 0.29 | <0.01 | 0.31 | <0.01 |
| | interaction | 0.03 | 0.95 | | |
| P₄ | EDJ area | 0.14 | <0.01 | | |
| | groups (genera) | 0.11 | <0.01 | 0.21 | <0.01 |
| | interaction | 0.04 | 0.73 | | |
| M₁ | EDJ area | 0.07 | <0.01 | | |
| | groups (genera) | 0.12 | <0.01 | 0.15 | <0.01 |
| | interaction | 0.05 | 0.18 | | |
| M₂ | EDJ area | 0.07 | <0.01 | | |
| | groups (genera) | 0.12 | <0.01 | 0.17 | <0.01 |
| | interaction | 0.04 | 0.38 | | |
| M₃ | EDJ area | 0.10 | <0.01 | | |
| | groups (genera) | 0.12 | <0.01 | 0.19 | <0.01 |
| | interaction | 0.05 | 0.31 | | |

Table S6. Presence/absence and degree of expression frequencies of the upper molar cusps 5 and 6 (UM C5 and UM C6), protoconule, Carabelli trait, and lower molar distal accessory cusp (DAC), lingual accessory cusp (LAC), mid-trigonid crest and protostyloid assessed on the EDJ. The darker green cells are those with higher frequencies. AUST: *Australopithecus*; HOM: Early and Middle Pleistocene *Homo*; PAR: *Paranthropus*. Significant values are highlighted in bold. Ent: entoconid type; Hld: hypoconulid type; Int: interconulid type; Med: metaconid type (for more information regarding scoring of each trait, see Supplementary Material and Methods).

| UM C5 | | n | M ¹ (%) | | | | M ² (%) | | | | M ³ (%) | | | |
|--------------------|---|---|--------------------|-------------|--------------------|-------------|--------------------|-------------|-------------|------|--------------------|-------------|-------------|------|
| taxon | (M ¹ , M ² , M ³) | | 0 | 0.5 | 1 | 2 | 0 | 0.5 | 1 | 2 | 0 | 0.5 | 1 | 2 |
| AUST | 14,9,11 | | 92.9 | 7.1 | 0.0 | 0.0 | 88.9 | 11.1 | 0.0 | 0.0 | 27.3 | 9.1 | 45.5 | 18.2 |
| HOM | 10,7,6 | | 90.0 | 10.0 | 0.0 | 0.0 | 100.0 | 0.0 | 0.0 | 0.0 | 83.3 | 0.0 | 16.7 | 0.0 |
| PAR | 12,10,9 | | 91.7 | 0.0 | 8.3 | 0.0 | 90.0 | 10.0 | 0.0 | 0.0 | 44.4 | 22.2 | 33.3 | 0.0 |
| UM C6 | | n | M ¹ (%) | | M ² (%) | | M ³ (%) | | | | | | | |
| taxon | (M ¹ , M ² , M ³) | | 0 | 1 | 0 | 1 | 0 | 1 | | | | | | |
| AUST | 14,9,11 | | 100.0 | 0.0 | 100.0 | 0.0 | 100.0 | 0.0 | | | | | | |
| HOM | 10,7,6 | | 100.0 | 0.0 | 100.0 | 0.0 | 100.0 | 0.0 | | | | | | |
| PAR | 12,10,9 | | 100.0 | 0.0 | 100.0 | 0.0 | 77.8 | 22.2 | | | | | | |
| protoconule | | n | M ¹ (%) | | | | M ² (%) | | | | M ³ (%) | | | |
| taxon | (M ¹ , M ² , M ³) | | 0 | 0.5 | 1 | 2 | 0 | 0.5 | 1 | 2 | 0 | 0.5 | 1 | 2 |
| AUST | 14,9,11 | | 78.6 | 21.4 | 0.0 | 0.0 | 100.0 | 0.0 | 0.0 | 0.0 | 72.7 | 27.3 | 0.0 | 0.0 |
| HOM | 10,7,6 | | 50.0 | 10.0 | 30.0 | 10.0 | 50.0 | 50.0 | 0.0 | 0.0 | 50.0 | 33.3 | 16.7 | 0.0 |
| PAR | 12,10,9 | | 58.3 | 25.0 | 16.7 | 0.0 | 100.0 | 0.0 | 0.0 | 0.0 | 55.6 | 22.2 | 22.2 | 0.0 |
| Carabelli trait | | n | M ¹ (%) | | | | M ² (%) | | | | M ³ (%) | | | |
| taxon | (M ¹ , M ² , M ³) | | 0 | 1 | 2 | 3 | 0 | 1 | 2 | 3 | 0 | 1 | 2 | 3 |
| AUST | 14,9,11 | | 28.6 | 28.6 | 28.6 | 14.3 | 11.1 | 33.3 | 55.6 | 0.0 | 9.1 | 72.7 | 18.2 | 0.0 |
| HOM | 10,7,6 | | 30.0 | 50.0 | 20.0 | 0.0 | 83.3 | 0.0 | 16.7 | 0.0 | 50.0 | 33.3 | 16.7 | 0.0 |
| PAR | 12,10,9 | | 25.0 | 58.3 | 16.7 | 0.0 | 30.0 | 70.0 | 0.0 | 0.0 | 11.1 | 33.3 | 44.4 | 11.1 |
| DAC | | n | M ₁ (%) | | | | M ₂ (%) | | | | M ₃ (%) | | | |
| taxon | (M ₁ , M ₂ , M ₃) | | none | Ent | Int | Hld | none | Ent | Int | Hld | none | Ent | Int | Hld |
| AUST | 19,25,18 | | 84.2 | 0.0 | 15.8 | 0.0 | 56.0 | 0.0 | 32.0 | 12.0 | 22.2 | 66.7 | 0.0 | 11.1 |
| HOM | 8,12,8 | | 75.0 | 0.0 | 12.5 | 12.5 | 41.7 | 0.0 | 33.3 | 25.0 | 75.0 | 0.0 | 25.0 | 0.0 |
| PAR | 17,14,16 | | 47.1 | 0.0 | 47.1 | 5.9 | 7.1 | 7.1 | 85.7 | 0.0 | 0.0 | 6.3 | 93.8 | 0.0 |
| LAC | | n | M ₁ (%) | | | | M ₂ (%) | | | | M ₃ (%) | | | |
| taxon | (M ₁ , M ₂ , M ₃) | | none | Med | Int | Ent | none | Med | Int | Ent | none | Med | Int | Ent |
| AUST | 19,25,18 | | 89.5 | 0.0 | 5.3 | 5.3 | 76.0 | 16.0 | 0.0 | 8.0 | 55.6 | 16.7 | 27.8 | 0.0 |
| HOM | 8,12,8 | | 37.5 | 62.5 | 0.0 | 0.0 | 66.7 | 8.3 | 25.0 | 0.0 | 50.0 | 25.0 | 25.0 | 0.0 |
| PAR | 17,14,16 | | 94.1 | 5.9 | 0.0 | 0.0 | 92.9 | 7.1 | 0.0 | 0.0 | 81.3 | 0.0 | 18.8 | 0.0 |
| mid-trigonid crest | | n | M ₁ (%) | | | | M ₂ (%) | | | | M ₃ (%) | | | |
| taxon | (M ₁ , M ₂ , M ₃) | | 0 | 1 | 2 | 3 | 0 | 1 | 2 | 3 | 0 | 1 | 2 | 3 |
| AUST | 19,25,18 | | 47.4 | 15.8 | 36.8 | 0.0 | 40.0 | 40.0 | 20.0 | 0.0 | 16.7 | 55.6 | 22.2 | 5.6 |
| HOM | 8,12,8 | | 25.0 | 37.5 | 25.0 | 12.5 | 50.0 | 33.3 | 16.7 | 0.0 | 50.0 | 37.5 | 12.5 | 0.0 |
| PAR | 17,14,16 | | 11.8 | 35.3 | 52.9 | 0.0 | 28.6 | 71.4 | 0.0 | 0.0 | 68.8 | 31.3 | 0.0 | 0.0 |
| protostyloid | | n | M ₁ (%) | | | | M ₂ (%) | | | | M ₃ (%) | | | |
| taxon | (M ₁ , M ₂ , M ₃) | | 0 | 1 | 2 | 0 | 1 | 2 | 0 | 1 | 2 | | | |
| AUST | 19,25,18 | | 0.0 | 10.5 | 89.5 | 4.0 | 32.0 | 64.0 | 0.0 | 22.2 | 77.8 | | | |
| HOM | 8,12,8 | | 75.0 | 12.5 | 12.5 | 58.3 | 25.0 | 16.7 | 75.0 | 25.0 | 0.0 | | | |
| PAR | 17,14,16 | | 0.0 | 0.0 | 100.0 | 0.0 | 28.6 | 71.4 | 12.5 | 6.3 | 81.3 | | | |

Table S7. Results of the permutational ANOVA testing the group differences based on size (log EDJ surface area). AUST: *Australopithecus*; HOM: Early and Middle Pleistocene *Homo*; PAR: *Paranthropus*. Significant values are highlighted in bold.

| tooth | groups compared | R ² | adjusted p-value |
|----------------------|-----------------|----------------|------------------|
| M¹ | AUST vs. HE | 0.06 | 0.52 |
| | AUST vs. PROB | 0.02 | 0.57 |
| | HE vs. PROB | 0.19 | 0.15 |
| M² | AUST vs. HE | 0.37 | 0.03 |
| | AUST vs. PROB | 0.01 | 0.86 |
| | HE vs. PROB | 0.37 | 0.02 |
| M³ | AUST vs. HE | 0.79 | <0.01 |
| | AUST vs. PROB | 0.09 | 0.18 |
| | HE vs. PROB | 0.86 | <0.01 |
| P₃ | AUST vs. HE | 0.19 | 0.10 |
| | AUST vs. PROB | 0.12 | 0.13 |
| | HE vs. PROB | 0.35 | 0.04 |
| P₄ | AUST vs. HE | 0.54 | <0.01 |
| | AUST vs. PROB | 0.27 | 0.01 |
| | HE vs. PROB | 0.71 | <0.01 |
| M₁ | AUST vs. HE | 0.32 | <0.01 |
| | AUST vs. PROB | 0.07 | 0.11 |
| | HE vs. PROB | 0.64 | <0.01 |
| M₂ | AUST vs. HE | 0.59 | <0.01 |
| | AUST vs. PROB | 0.05 | 0.16 |
| | HE vs. PROB | 0.71 | <0.01 |
| M₃ | AUST vs. HE | 0.55 | <0.01 |
| | AUST vs. PROB | 0.08 | 0.12 |
| | HE vs. PROB | 0.79 | <0.01 |

Table S8. Results of the bgPCA (left) and CVA (right) of size (log EDJ area) showing typicality probabilities of the investigated specimens. For each specimen, typicality probabilities are shown only for the group to which that specimen is affiliated. AUST: *Australopithecus*; HOM: Early and Middle Pleistocene *Homo*; PAR: *Paranthropus*.

| | HOM | AUS | PAR |
|----------------------|-----------|--------|-----------|
| M¹ | | | |
| DNH 39 | -/0.92 | -/- | 0.97/- |
| DNH 62 | -/0.91 | -/- | 0.73/- |
| DNH 70 | 0.81/0.50 | -/- | -/- |
| SE 255 | -/0.75 | 0.87/- | -/- |
| SK 27 L | -/- | -/0.95 | 0.22/- |
| SK 27 R | -/- | -/- | 0.17/0.94 |
| SKX 268 | 0.86/0.52 | -/- | -/- |
| StW 151 L | 0.42/0.32 | -/- | -/- |
| StW 151 R | 0.71/0.46 | -/- | -/- |
| StW 669 | 0.99/0.60 | -/- | -/- |
| M² | | | |
| SE 1508 | 0.41/0.76 | -/- | -/- |
| SK 27 | -/0.46 | 0.35/- | -/- |
| StW 151 | 0.65/0.83 | -/- | -/- |
| M³ | | | |
| SK 847 | 0.07/- | -/0.17 | -/- |
| StW 19 | 0.14/- | -/0.13 | -/- |
| StW 53 L | -/- | -/0.99 | 0.66/- |
| StW 53 R | -/- | -/0.97 | 0.57/- |
| P₃ | | | |
| SK 18a | -/0.82 | 0.80/- | -/- |
| SK 96 | -/0.97 | 0.96/- | -/- |
| SKX 21204 | 0.73/0.23 | -/- | -/- |
| StW 80 | -/- | -/0.77 | 0.42/0.77 |
| P₄ | | | |
| SK 18a | 0.32/0.97 | -/- | -/- |
| SKX 21204 | 0.33/0.96 | -/- | -/- |
| StW 80 | -/0.27 | -/- | 0.49/- |
| StW 87 | 0.64/0.81 | -/- | -/- |
| StW 151 L | -/0.83 | 0.50/- | -/- |
| StW 151 R | -/0.27 | -/- | 0.50/- |
| M₁ | | | |
| DNH 67 | -/- | -/0.77 | 0.70/- |
| KB 5223 | -/- | -/0.69 | 0.82/- |
| SKX 257 | -/0.79 | 0.60/- | -/- |

| | | | |
|----------------------|-----------|-----------|-----------|
| Sts 9 | -/- | -/0.94 | 0.49/- |
| StW 151 L | 0.85/0.73 | -/- | -/- |
| StW 151 R | 0.92/0.68 | -/- | -/- |
| M₂ | | | |
| SK 15 | -/- | -/- | 0.89/0.44 |
| StW 80 | 0.34/0.37 | -/- | -/- |
| M₃ | | | |
| SK 15 L | -/- | -/- | 0.73/0.92 |
| SK 15 R | -/- | -/- | 0.65/0.89 |
| StW 53h | -/- | 0.29/0.97 | -/- |
| StW 81 | 0.54/- | -/0.69 | -/- |

SI References

1. R. Broom, J. T. Robinson, A new type of Man. *Nature* **164**, 322-323 (1949).
2. J. T. Robinson, The Australopithecines and their bearing on the origin of Man and of stone tool-making. *South Afr. J. Sci.* **57**, 3-13 (1961).
3. J. T. Robinson, *Telanthropus* and its phylogenetic significance. *Am. J. Phys. Anthropol.* **111**, 445-501 (1953).
4. F. E. Grine, New hominid fossils from the Swartkrans Formation (1979-1986 excavations): Craniodental specimens. *Am. J. Phys. Anthropol.* **79**, 409-449 (1989).
5. R. J. Clarke, A juvenile cranium and some adult teeth of early *Homo* from Swartkrans, Transvaal. *S. Afr. J. Sci.* **73**, 46-49 (1977).
6. R. J. Clarke, F. C. Howell, C. K. Brain, More evidence of an advanced hominid at Swartkrans. *Nature* **225**, 1219-1222 (1970).
7. F. E. Grine, H. F. Smith, C. P. Heesy, E. J. Smith, "Phenetic affinities of Plio-Pleistocene *Homo* fossils from South Africa: Molar cusp proportions" in *The First Humans - Origin and Early Evolution of the Genus Homo*, F. E. Grine, J. G. Fleagle, R. E. Leakey, Eds. (Springer, New York, 2009), pp. 49-62.
8. B. A. Wood, *Wiley-Blackwell Encyclopedia of Human Evolution* (Blackwell Publishing, Chichester, 2011).
9. T. W. Davies *et al.*, Distinct mandibular premolar crown morphology in *Homo naledi* and its implications for the evolution of *Homo* species in southern Africa. *Sci. Rep.* **10**, 13196 (2020).
10. J. Braga, J. F. Thackeray, Early *Homo* at Kromdraai B: probabilistic and morphological analysis of the lower dentition. *C. R. Palevol* **2**, 269-279 (2003).
11. A.W. Keyser, C. G. Menter, J. Moggi-Cecchi, T. R. Pickering, L. R. Berger, Drimolen: a new hominid-bearing site in Gauteng, South Africa. *S. Afr. J. Sci.* **96**, 193-197 (2000).
12. J. Moggi-Cecchi, C. Menter, S. Boccone, A. Keyser, Early hominin dental remains from the Plio-Pleistocene site of Drimolen, South Africa. *J. Hum. Evol.* **58**, 374-405 (2010).
13. J. Moggi-Cecchi, F. E. Grine, P. V. Tobias, Early hominid dental remains from Members 4 and 5 of the Sterkfontein Formation (1966–1996 excavations): catalogue, individual associations, morphological descriptions and initial metrical analysis. *J. Hum. Evol.* **50**, 239-328 (2006).
14. R. Couzens, Spatial Modelling, Formation and Transformation of the Oldowan Lithic Artefact Assemblages from Sterkfontein Caves, South Africa. Ph.D. Dissertation (University of the Witwatersrand, Johannesburg, 2021).
15. P. V. Tobias, The earliest Transvaal members of the genus *Homo* with another look at some problems of hominid taxonomy and systematics. *Z. Morphol. Anthropol.* **69**, 225-265 (1978).
16. P.V. Tobias, *Australopithecus*, *Homo habilis*, tool-using, and tool-making. *S. Afr. Archaeol. Bull.* **20**, 167-192 (1965).
17. K. Kuman, R. J. Clarke, Stratigraphy, artefact industries and hominid associations for Sterkfontein, Member 5. *J. Hum. Evol.* **38**, 827-847 (2000).
18. D. Stratford, J. L. Heaton, T. R. Pickering, M. V. Caruana, K. Shadrach, First hominin fossils from Milner Hall, Sterkfontein, South Africa. *J. Hum. Evol.* **91**, 167-173 (2016).
19. B. Mataboge, A. Beaudet, J. L. Heaton, T.R. Pickering, D. Stratford, Endostructural assessment of a hominin maxillary molar (StW 669) from Milner Hall, Sterkfontein, South Africa. *S. Afr. J. Sci.* **115**, 6404 (2019).
20. G. R. Scott, J. D. Irish, *Human Tooth Crown and Root Morphology. The Arizona State University Dental Anthropology System* (Cambridge University Press, Cambridge, 2017).
21. S.E. Bailey, J.-J. Hublin, "What does it mean to be dentally "modern"?" in *Anthropological Perspectives on Tooth Morphology. Genetics, Evolution, Variation*, G. R. Scott, J. D. Irish, Eds. (Cambridge University Press, Cambridge, 2013), pp. 222-249.
22. C. Zanolli, Brief Communication: Molar crown inner structural organization in Javanese *Homo erectus*. *Am. J. Phys. Anthropol.* **156**, 148-157 (2015).

23. R. A. Dart, *Australopithecus africanus*: The man-ape of South Africa. *Nature* **115**, 195–199 (1925).
24. R. Broom, Pleistocene anthropoid apes of South Africa. *Nature* **142**, 377-379 (1938).
25. R. J. Clarke, K. Kuman, The skull of StW 573, a 3.67 Ma *Australopithecus prometheus* skeleton from Sterkfontein Caves, South Africa. *J. Hum. Evol.* **134**, 102634 (2019).
26. J. W. Hoffman, F. de Beer, "Characteristics of the micro-focus X-ray tomography facility (MIXRAD) at Necsa in South Africa" in *18th World Conference on Nondestructive Testing, 16-20 April 2012, Durban, South Africa*.
27. C. Zanolli *et al.*, When X-rays do not work. Characterizing the internal structure of fossil hominid dentognathic remains using high-resolution neutron microtomographic imaging. *Front. Ecol. Evol.* **8**, 42 (2020).
28. C. F. Spoor, F. W. Zonneveld, G. A. Macho, Linear measurements of cortical bone and dental enamel by computed tomography: Applications and problems. *Am. J. Phys. Anthropol.* **91**, 469-484 (1993).
29. R. S. Fajardo, T. M. Ryan, J. Kappelman, Assessing the accuracy of high-resolution X-ray computed tomography of primate trabecular bone by comparisons with histological sections. *Am. J. Phys. Anthropol.* **118**, 1-10 (2002).
30. M. N. Coleman, M. W. Colbert, Technical Note: CT thresholding protocols for taking measurements on three-dimensional models. *Am. J. Phys. Anthropol.* **133**, 723-725 (2007).
31. A. Ortiz, S. E. Bailey, G. T. Schwartz, J.-J. Hublin, M. M. Skinner, Evo-devo models of tooth development and the origin of hominoid molar diversity. *Sci. Adv.* **4**, eaar2334 (2018).
32. S. E. Bailey, M. M. Skinner, J.-J. Hublin, What lies beneath? An evaluation of lower molar trigonid crest patterns based on both dentine and enamel expression. *Am. J. Phys. Anthropol.* **145**, 505-518 (2011).
33. T. W. Davies *et al.*, Accessory cusp expression at the enamel-dentine junction of hominin mandibular molars. *PeerJ* **9**, e11415 (2021).
34. M.M. Skinner *et al.*, Dental trait expression at the enamel-dentine junction of lower molars in extant and fossil hominoids. *J. Hum. Evol.* **54**, 173-186 (2008).
35. J. Glaunès, S. Joshi, "Template Estimation from Unlabeled Point Set Data and Surfaces for Computational Anatomy" in *Proceedings of the International Workshop on the Mathematical Foundations of Computational Anatomy*, X. Pennec, S. Joshi, Eds. (LNCS Springer, Copenhagen, 2006), pp. 29-39.
36. S. Durrleman *et al.*, Morphometry of anatomical shape complexes with dense deformations and sparse parameters. *NeuroImage* **101**, 35-49 (2014).
37. S. Durrleman, X. Pennec, A. Trouvé, N. Ayache, J. Braga, Comparison of the endocranial ontogenies between chimpanzees and bonobos via temporal regression and spatiotemporal registration. *J. Hum. Evol.* **62**, 74-88 (2012).
38. A. Beaudet *et al.*, Morphoarchitectural variation in South African fossil cercopithecoid endocasts. *J. Hum. Evol.* **101**, 65-78 (2016).
39. C. Zanolli *et al.*, Inner tooth morphology of *Homo erectus* from Zhoukoudian. New evidence from an old collection housed at Uppsala University, Sweden. *J. Hum. Evol.* **116**, 1-13 (2018).
40. A. Urciuoli *et al.*, Reassessment of the phylogenetic relationships of the late Miocene apes *Hispanopithecus* and *Rudapithecus* based on vestibular morphology. *Proc. Natl. Acad. Sci. U.S.A.* **118**, e2015215118 (2021).
41. J. Braga *et al.*, Efficacy of diffeomorphic surface matching and 3D geometric morphometrics for taxonomic discrimination of Early Pleistocene hominin mandibular molars. *J. Hum. Evol.* **130**, 21-35 (2019).
42. L. Pan, J. Dumoncel, A. Mazurier, C. Zanolli, Hominin diversity in East Asia during the Middle Pleistocene: A premolar endostructural perspective. *J. Hum. Evol.* **148**, 102888 (2020).
43. J. Dumoncel, *RToolsForDeformetrica* (R package version 0.1, 2021). https://gitlab.com/jeandumoncel/tools-for-deformetrica/-/tree/master/src/R_script/RToolsForDeformetrica. Accessed 30 April 2021.

44. S. Dray, A. Dufour, The ade4 package: implementing the duality diagram for ecologists. *J. Stat. Softw.* **22**, 1-20 (2007).
45. S. Schlager, "Morpho and Rvcg—Shape analysis in R" in *Statistical Shape and Deformation Analysis*, G. Zheng, S. Li, G. Szekely, Eds. (Academic Press, 2017), pp. 217-256.
46. R Core-Team, *R: A Language and Environment for Statistical Computing* (R Foundation for Statistical Computing, Vienna, Austria, 2021).
47. A. Cardini, P. D. Polly, Cross-validated between group PCA scatterplots: A solution to spurious group separation? *Evol. Biol.* **47**, 85-95 (2020).
48. T. Hastie, R. Tibshirani, J. Friedman, *The Elements of Statistical Learning, Second Edition* (Springer, New York, 2009).
49. M.M. Skinner, P. Gunz, B. A. Wood, C. Boesch, J.-J. Hublin, Discrimination of extant *Pan* species and subspecies using the enamel-dentine junction morphology of lower molars. *Am. J. Phys. Anthropol.* **140**, 234-243 (2009).
50. J. Oksanen *et al.*, *vegan: Community ecology package* (R package version 2.5-7, 2020). <https://CRAN.R-project.org/package=vegan>. Accessed 15 March 2021.
51. P. Martinez Arbizu, *pairwiseAdonis: Pairwise multilevel comparison using adonis* (R package version 0.4, 2020). <https://github.com/pmartinezarbizu/pairwiseAdonis>. Accessed 15 March 2021.
52. A. Cardini, P. O'Higgins, F. J. Rohlf, Seeing distinct groups where there are none: Spurious patterns from between-group PCA. *Evol. Biol.* **46**, 303-316 (2019).
53. F. L. Bookstein, *Morphometric Tools for Landmark Data: Geometry and Biology* (Cambridge University Press, Cambridge, 1991).
54. C. Austin *et al.*, Uncovering system-specific stress signatures in primate teeth with multimodal imaging. *Sci. Rep.* **6**, 18802 (2016).
55. R. Joannes-Boyau *et al.*, Elemental signatures of *Australopithecus africanus* teeth reveal seasonal dietary stress. *Nature* **572**, 112-115 (2019).
56. M. Niedzwiecki *et al.*, A multimodal imaging workflow to visualize metal mixtures in the human placenta and explore colocalization with biological response markers. *Metallomics* **8**, 444-452 (2016).
57. F. E. Grine, A new juvenile hominid (Mammalia: Primates) from Member 3, Kromdraai Formation, Transvaal, South Africa. *Ann. Transvaal Mus.* **33**, 165-239 (1982).
58. J. T. Robinson, Australopithecines and artefacts at Sterkfontein - Part I Sterkfontein stratigraphy and the significance of the Extension Site. *S. Afr. Archaeol. Bull.* **17**, 87-107 (1962).
59. A. R. Hughes, P. V. Tobias, A fossil skull probably of the genus *Homo* from Sterkfontein, Transvaal. *Nature* **265**, 310-312 (1977).
60. J. Moggi-Cecchi, P. V. Tobias, A. D. Beynon, The mixed dentition and associated skull fragments of a juvenile fossil hominid from Sterkfontein, South Africa. *Am. J. Phys. Anthropol.* **106**, 425-465 (1998).
61. J. T. Robinson, The dentition of the Australopithecinae. *Mem. Transvaal Mus.* **9**, 1-179 (1956).
62. ESRF heritage database for palaeontology, evolutionary biology and archaeology (2021). <http://paleo.esrf.eu>.
63. I. Crevecoeur *et al.*, First early hominin from Central Africa (Ishango, Democratic Republic of Congo). *PLoS ONE* **9**, e84652 (2014).
64. A. L. Lockey, Z. Alemseged, J.-J. Hublin, M. M. Skinner, Maxillary molar enamel thickness of Plio-Pleistocene hominins. *J. Hum. Evol.* **142**, 102731 (2020).
65. C. Zanolli *et al.*, Evidence for increased hominid diversity in the Early to Middle Pleistocene of Indonesia. *Nature Ecol. Evol.* **3**, 755-764 (2019).
66. L. Pan, C. Zanolli, Comparative observations on the premolar root and pulp canal configurations of Middle Pleistocene *Homo* in China. *Am. J. Phys. Anthropol.* **168**, 637-646 (2019).

67. L. Pan, J. Dumoncel, A. Mazurier, C. Zanolli, Structural analysis of premolar roots in Middle Pleistocene hominins from China. *J. Hum. Evol.* **136**, 102669 (2019).
68. C. Zanolli, A. Mazurier, Endostructural characterization of the *H. heidelbergensis* dental remains from the early Middle Pleistocene site of Tighenif, Algeria. *C. R. Palevol* **12**, 293-304 (2013).
69. C. Zanolli *et al.*, Exploring hominin and non-hominin primate dental fossil remains with neutron microtomography. *Phys. Proc.* **88**, 109-115 (2017).
70. M. M. Skinner, Z. Alemseged, C. Gaunitz, J.-J. Hublin, Enamel thickness trends in Plio-Pleistocene hominin mandibular molars. *J. Hum. Evol.* **85**, 35-45 (2015).
71. C. Zanolli *et al.*, The late Early Pleistocene human dental remains from Uadi Aalad and Mulhuli-Amo (Buia), Eritrean Danakil: Macromorphology and microstructure. *J. Hum. Evol.* **74**, 96-113 (2014).
72. C. Zanolli, *L'organisation endostructurale de restes dentaires humains du Pléistocène inférieur final-moyen initial d'Indonésie et d'Afrique, avec une attention particulière à Homo erectus s.s. caractérisation comparative à haute résolution et problématiques taxinomiques*. Ph.D. Dissertation (Muséum National d'Histoire Naturelle, Paris, 2011).
73. S. Xing, M. Martinón-Torres, J. M. Bermúdez de Castro, The fossil teeth of the Peking Man. *Sci. Rep.* **8**, 2066 (2018).